SAND2022-6467C

Sandia National Laboratories

Securing the future of Nuclear Energy

MELCOR

MELCOR Integrated Severe Accident Code Demonstration and Sensitivity Study of HTGR Accident Progression

K.C. Wagner, B. Beeny, and D.L. Luxat
Nuclear Energy Safety Modeling and Analysis (8852)

Sandia National Laboratories is a multimission laboratory managed and operated by National Technology and Engineering Solutions of Sandia, LLC, a wholly owned subsidiary of Honeywell International Inc., for the U.S. Department of Energy's National Nuclear Security Administration under contract DE-NA0003525.

Sandia National Laboratories is a multimission laboratory managed and operated by National Technology and Engineering Solutions of Sandia, LLC, a wholly owned subsidiary of Honeywell International Inc., for the U.S. Department of Energy's National Nuclear Security Administration under contract DE-NA0003525.

MELCOR HTGR modeling

Fission product release

- Release from TRISO kernel
- Radionuclide distributions within the layers in the TRISO particle and compact
- Release to coolant

Other core models

- Graphite oxidation
- Intercell and intracell conduction
- Convection & flow
- Point kinetics
- Dust generation and resuspension

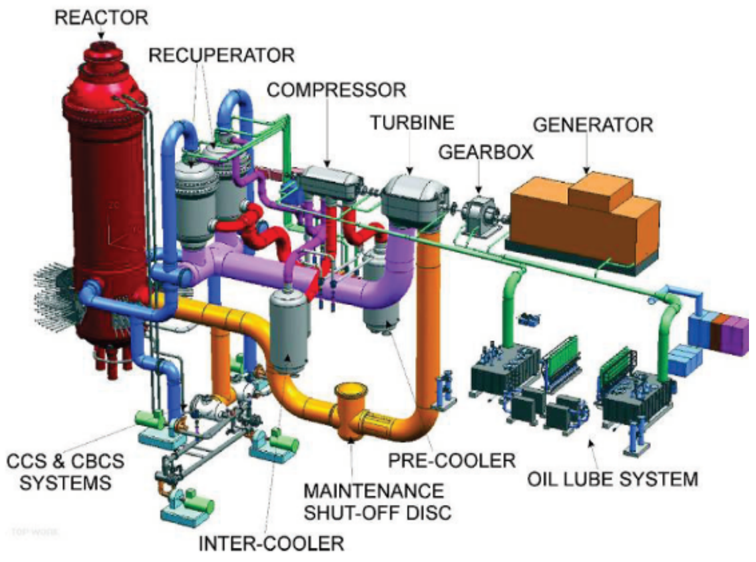

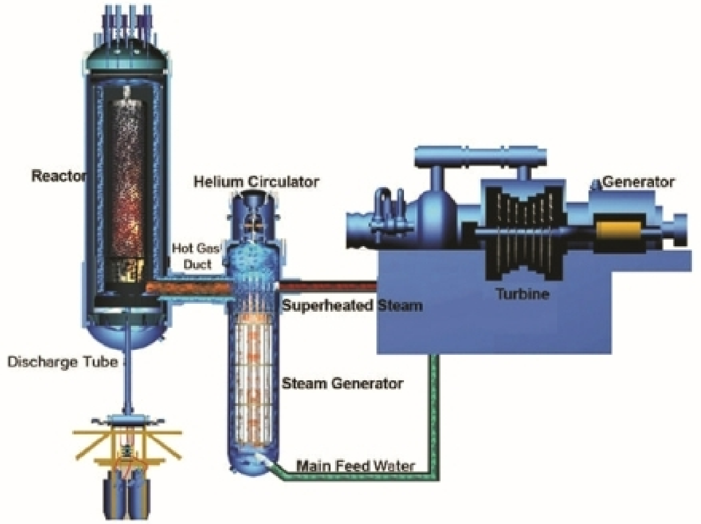

HTGR Components

MELCOR

- Pebble Bed Reactor Fuel/Matrix Components
  - Fueled part of pebble
  - Unfueled shell (matrix) is modeled as separate component
  - Fuel radial temperature profile for sphere

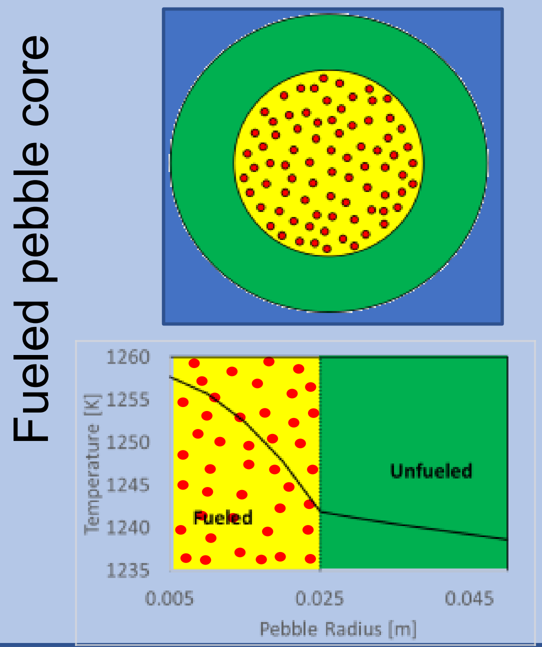

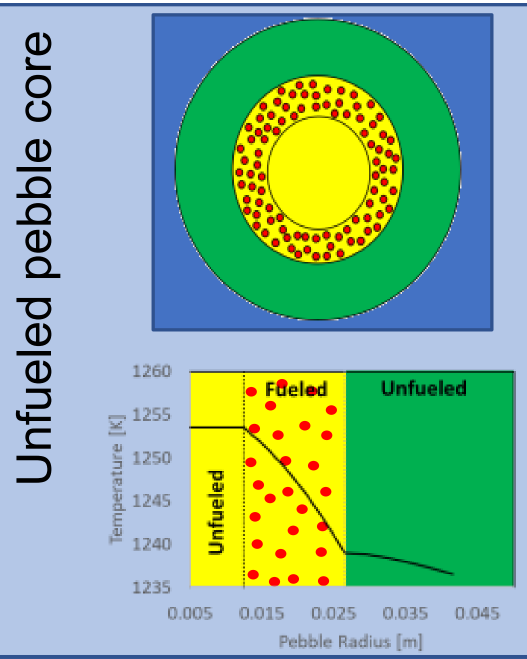

- Prismatic Modular Reactor Fuel/Matrix Components
  - "Rod-like" geometry
  - Part of hex block associated with a fuel channel is matrix component
  - Fuel radial temperature profile for cylinder

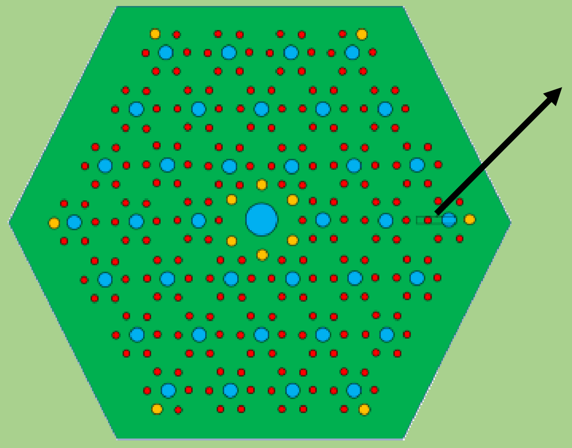

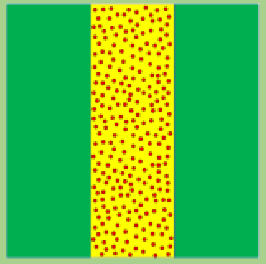

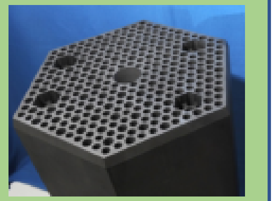

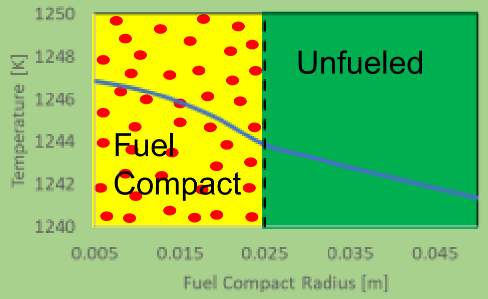

Legend

TRISO	Fuel (FU)
GRAPHITE	
GRAPHITE	Matrix (MX)
	Fluid B/C

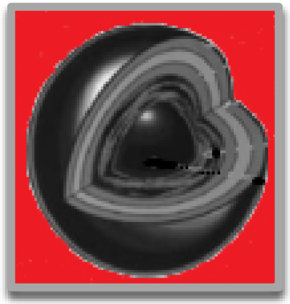

TRISO (FU)

Sub-component model for zonal diffusion of radionuclides through TRISO particle

Transient/Accident Solution Methodology

Stage 0:
Normal Operation
Establish thermal state

Time constant in HTGR graphite structures is very large

Reduce heat capacities for structures to reach steady state thermal conditions.

Reset heat capacities after steady state is achieved.

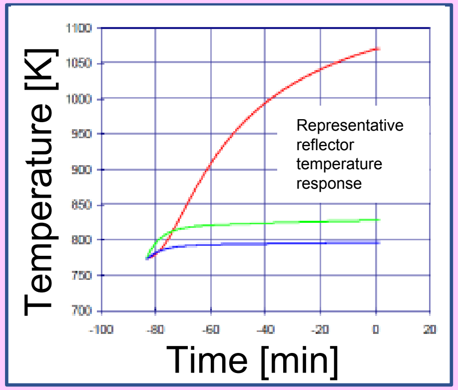

Stage 1:
Normal Operation
Diffusion Calculation

Establish steady state distribution of radionuclides <u>in TRISO particles and matrix</u>

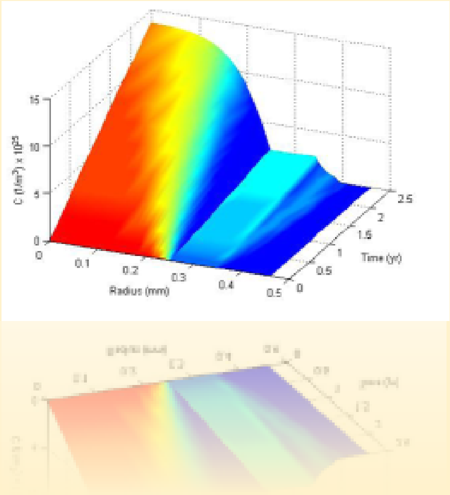

Stage 2:
Normal Operation
Transport Calculation

Calculate steady state distribution of radionuclides and graphite dust <u>throughout system</u> (deposition on surfaces, convection through flow paths)

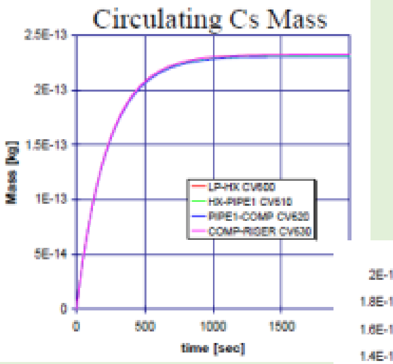

Example: PBMR -400 Cs Distribution in Primary System

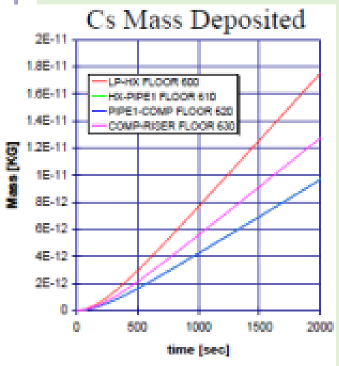

Stage 3:
Accident
Diffusion & Transport calculation

Calculate accident progression and radionuclide release

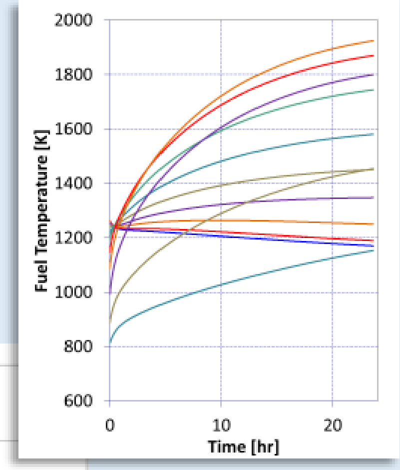

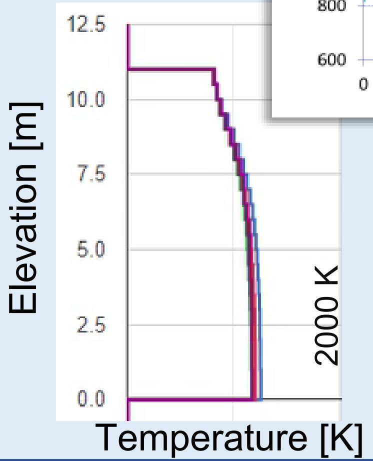

HTGR Radionuclide Diffusion Release Model

Intact TRISO Particles

- One-dimensional finite volume diffusion equation solver for multiple zones (materials)
- Temperature-dependent diffusion coefficients (Arrhenius form)

$$\frac{\partial C}{\partial t} = \frac{1}{r^n}\frac{\partial}{\partial r}\left(r^n D \frac{\partial C}{\partial r}\right) - \lambda C + \beta \qquad D(T) = D_0 e^{-\frac{Q}{RT}}$$

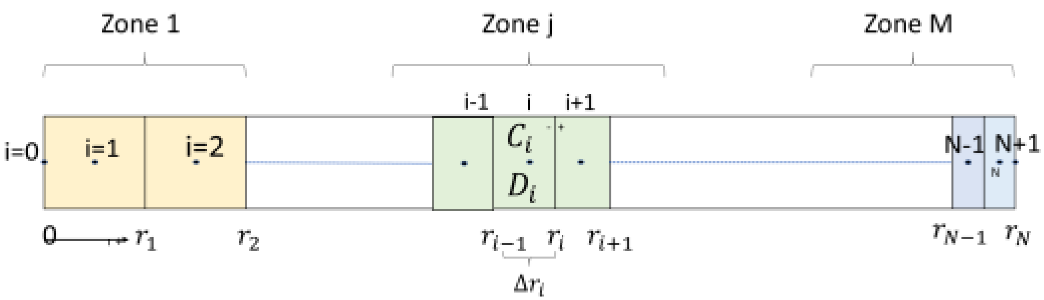

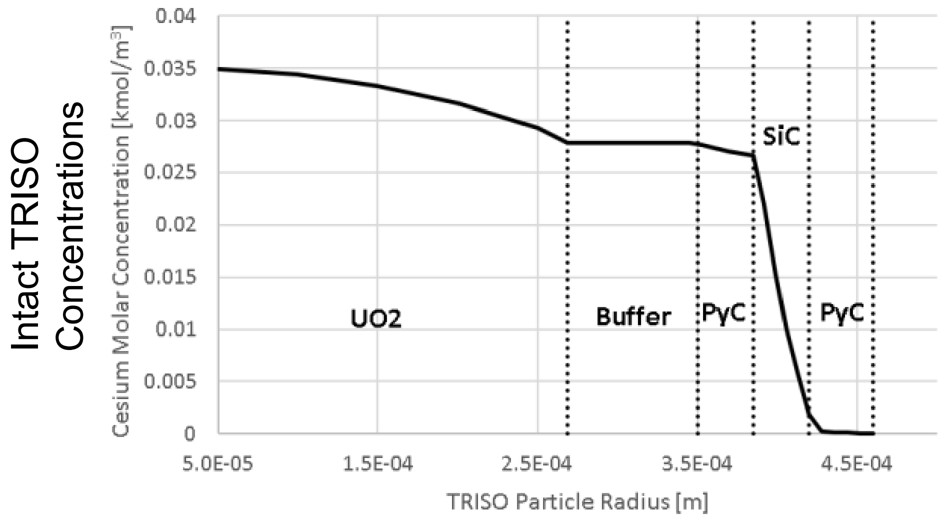

Diffusivity Data Availability

Radionuclide	UO_2	UCO	PyC	Porous Carbon	SiC	Matrix Graphite	TRISO Overall
Ag	Some	Not investigated	Some	Not found	Extensive	Some	Extensive
Cs	Some		Some		Extensive	Some	Some
I	Some		Some		Some	Not found	Not found
Kr	Some		Some		Not found	Some	Some
Sr	Some		Some		Extensive	Some	Some
Xe	Some		Some		Some	Some	Not found

Data used in the demo calculation

[IAEA TECDOC-0978]

Layer	FP Species							
	Kr		Cs		Sr		Ag	
	D (m^2/s)	Q (J/mole)	D (m^2/s)	Q (J/mole)	D (m^2/s)	Q (J/mole)	D (m2/s)	Q (J/mole)
Kernel (normal)	1.3E-12	126000.0	5.6-8	209000.0	2.2E-3	488000.0	6.75E-9	165000.0
Buffer	1.0E-8	0.0	1.0E-8	0.0	1.0E-8	0.0	1.0E-8	0.0
PyC	2.9E-8	291000.0	6.3E-8	222000.0	2.3E-6	197000.0	5.3E-9	154000.0
SiC	3.7E+1	657000.0	7.2E-14	125000.0	1.25E-9	205000.0	3.6E-9	215000.0
Matrix Carbon	6.0E-6	0.0	3.6E-4	189000.0	1.0E-2	303000.0	1.6E00	258000.0
Str. Carbon	6.0E-6	0.0	1.7E-6	149000.0	1.7E-2	268000.0	1.6E00	258000.0

Iodine assumed to behave like Kr

CORSOR-Booth LWR scaling used to estimate other radionuclides

HTGR Radionuclide Release Models

ELCOR

- Recent failures – particles failing within latest time-step (burst release, diffusion release in time-step)
- Previous failures – particles failing on a previous time-step (time history of diffusion release)
- Contamination and recoil

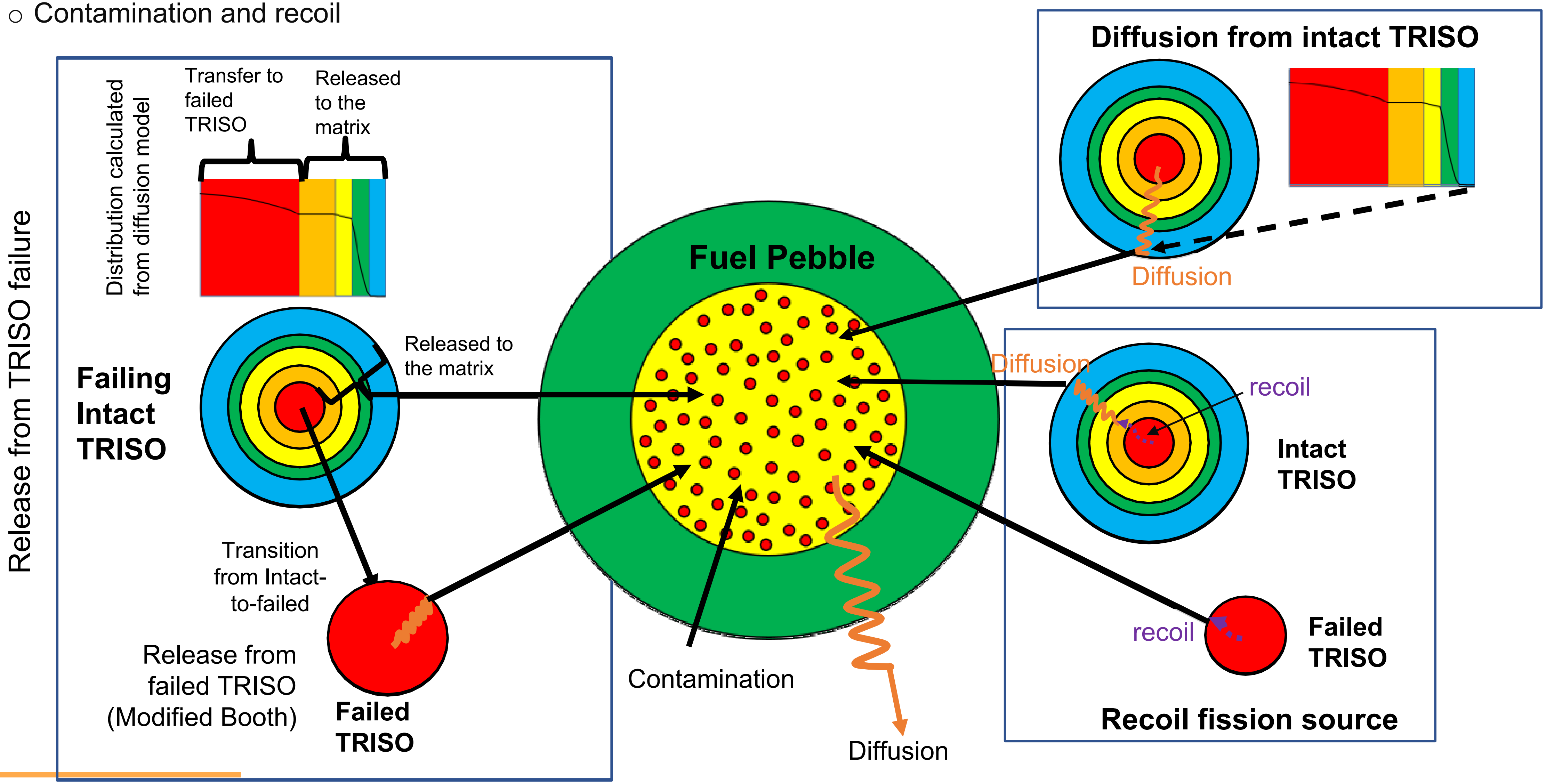

Graphite Oxidation

IIIELCOR

Steam oxidation

$$R_{OX,steam} = \frac{k_4 P_{H_2O}}{1 + k_5 P_{H_2}^{0.5} + k_6 P_{H_2O}}$$

Reactions

$C + H_2O(g) \rightarrow CO(g) + H_2(g)$
$CO(g) + H_2O(g) \rightarrow CO_2(g) + H_2(g)$

Air oxidation

$$R_{OX} = 1.7804x10^4 \exp\left(-\frac{20129}{T}\right)\left(\frac{P}{0.21228x10^5}\right)^{0.5}$$

Reactions

1. $C + O_2 \rightarrow CO_2(g)$
2. $C + \frac{1}{2}O_2 \rightarrow CO(g)$
3. $CO(g) + \frac{1}{2}O_2(g) \rightarrow CO_2(g)$
4. $C + CO_2(g) \rightarrow 2CO(g)$

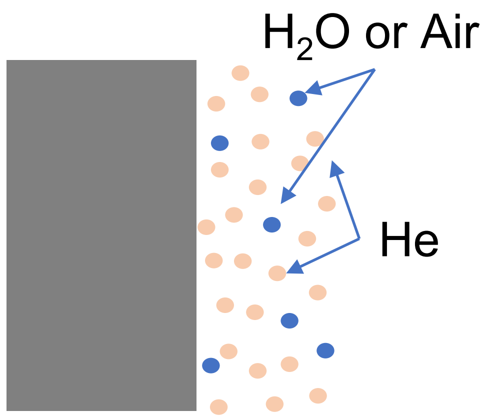

Both steam and air include rate limit due to steam/air diffusion towards active oxidation surface

R_{OX} is the rate term in the parabolic oxidation equation [1/s]

COR Intercell Conduction

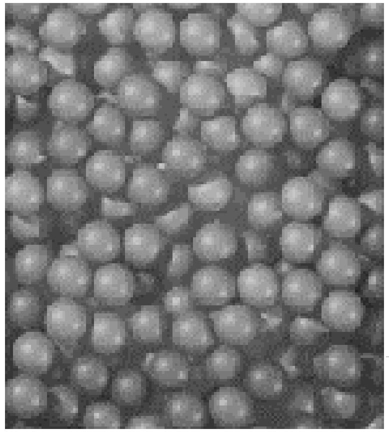

Effective conductivity prescription for pebble bed (bed conductance)

- Zehner-Schlunder-Bauer with Breitbach-Barthels modification to the radiation term

$$k_{eff} = \left(1-\sqrt{1-\varepsilon}\right)\varepsilon 4\sigma T^3 D_p + \left(1-\sqrt{1-\varepsilon}\right)k_f + \sqrt{1-\varepsilon}\, k_c(T, D_p, \varepsilon, k_f, k_s, k_r)$$

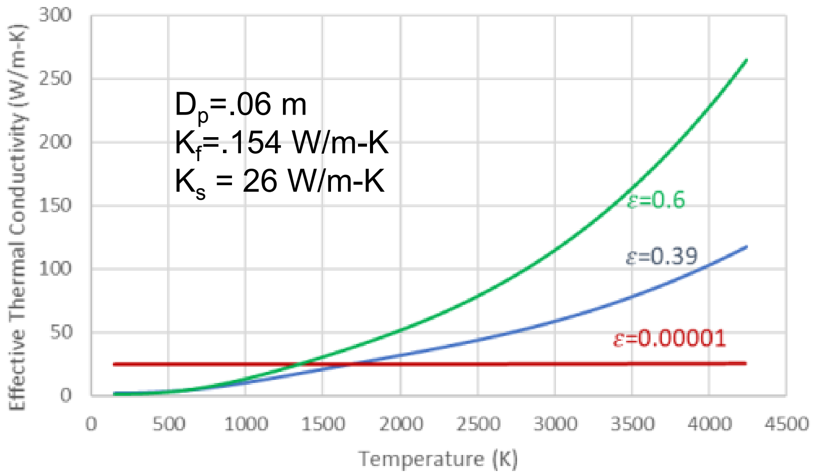

Effective conductivity prescription for prismatic (continuous solid with pores)

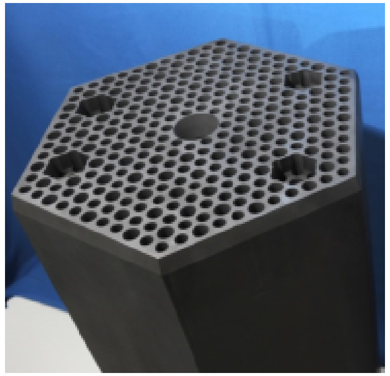

- Tanaka and Chisaka expression for effective radial conductivity (of a single PMR hex block)

$$k_{eff} = k_s\left[A + (1-A)\frac{\ln\left(1+2B\left(k_{por}/k_s - 1\right)\right)}{2B\left(1-k_s/k_{por}\right)}\right]$$

- A radiation term is incorporated in parallel with the pore conductivity
- Thermal resistance of helium gaps between hex block fuel elements is added in parallel via a gap conductance term

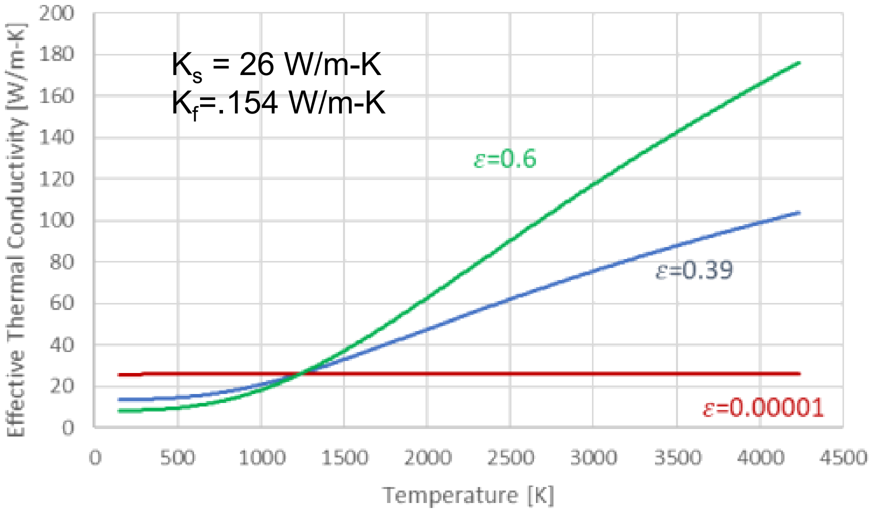

Interface Between Thermal-hydraulics and Pebble Bed Reactor Core Structures

MELCOR

Heat transfer coefficient (Nusselt number) correlations for pebble bed convection:

- Isolated, spherical particles
- Use T_{film} to evaluate non-dimensional numbers, use maximum of forced and free Nu

$$Nu_{Free} = 2.0 + 0.6\, Gr_f^{1/4}\, Pr_f^{1/3} \qquad Nu_{Forced} = 2.0 + 0.6\, Re_f^{1/2} Pr_f^{1/3}$$

- Constants and exponents accessible by sensitivity coefficient

Flow resistance

- Packed bed pressure drop

$$K_L(\varepsilon, Re) = \left[C_1 + C_2 \frac{1-\varepsilon}{Re} + C_3 \left(\frac{1-\varepsilon}{Re}\right)^{C_4}\right] \frac{(1-\varepsilon)}{\varepsilon D_p} L$$

Correlation	C_1	C_2	C_3	C_4
Ergun (original)	3.5	300.	0.0	-
Modified Ergun (smooth)	3.6	360.	0.0	-
Modified Ergun (rough)	8.0	360.	0.0	-
Achenbach	1.75	320.	20.0	0.4

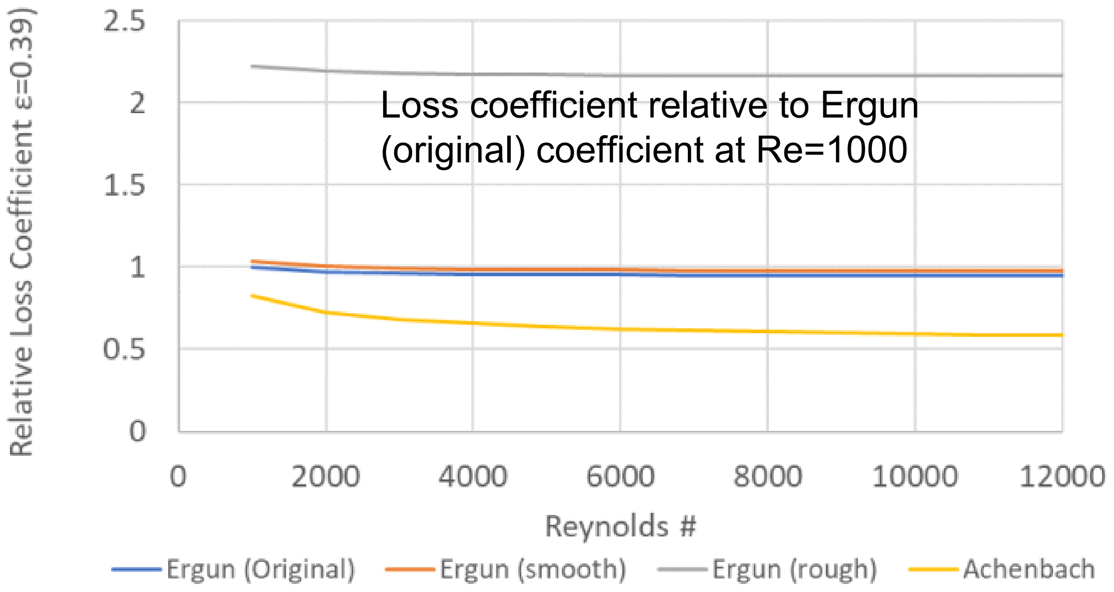

Point kinetics modeling

Standard treatment

$$\frac{dP}{dt} = \left(\frac{\rho - \beta}{\Lambda}\right) P + \sum_{i=1}^{6} \lambda_i Y_i + S_0$$

$$\frac{dY_i}{dt} = \left(\frac{\beta_i}{\Lambda}\right) P - \lambda_i C_i, \qquad for\ i = 1 \ldots 6$$

Feedback models

- User-specified external input
- Doppler
- Fuel and moderator density

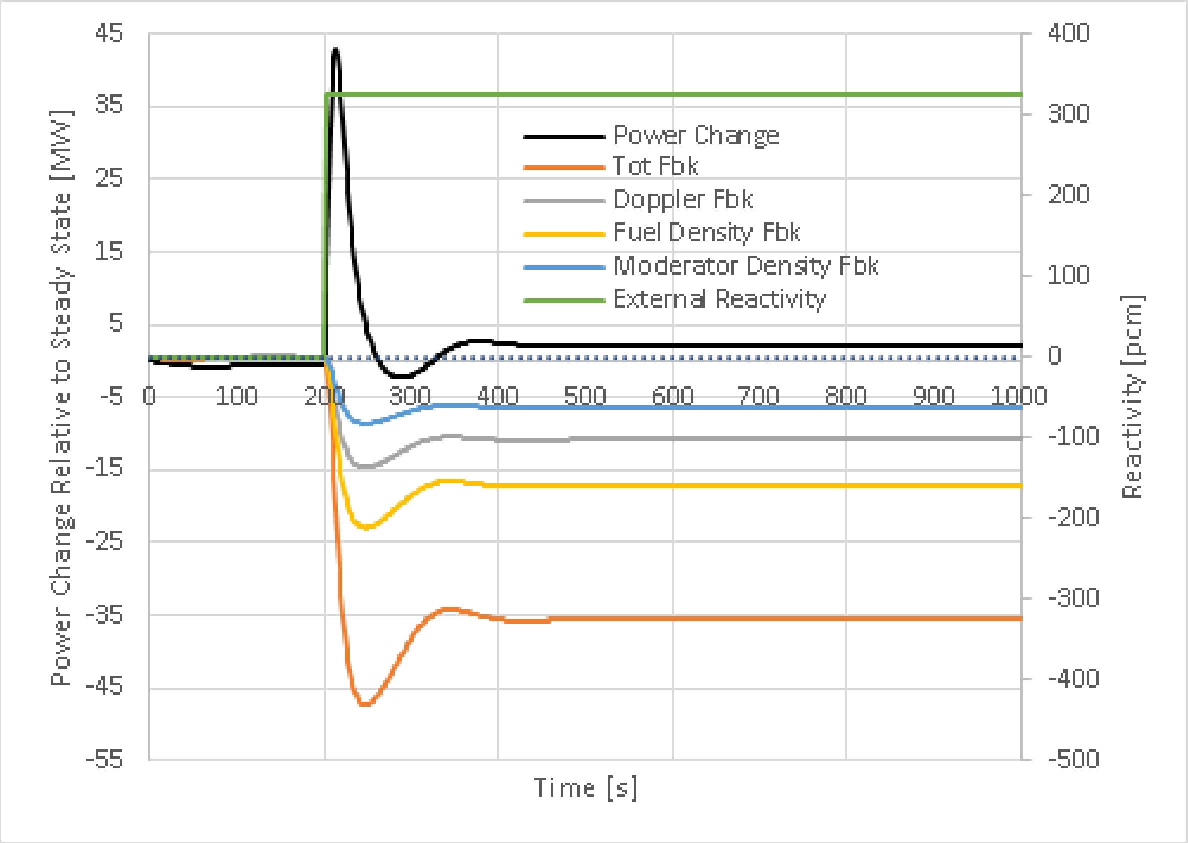

Reactor vessel and core

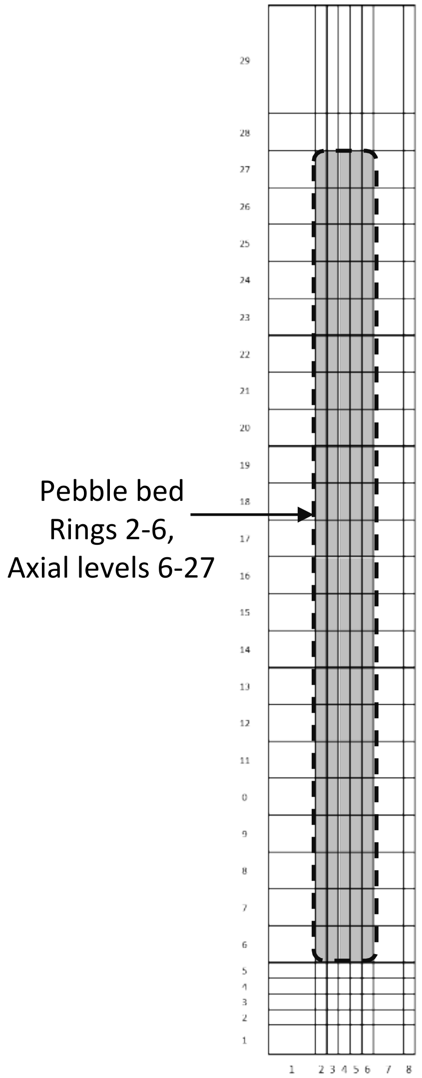

Vessel core package nodalization
(8 rings x 29 axial levels)
Correct aspect ratio

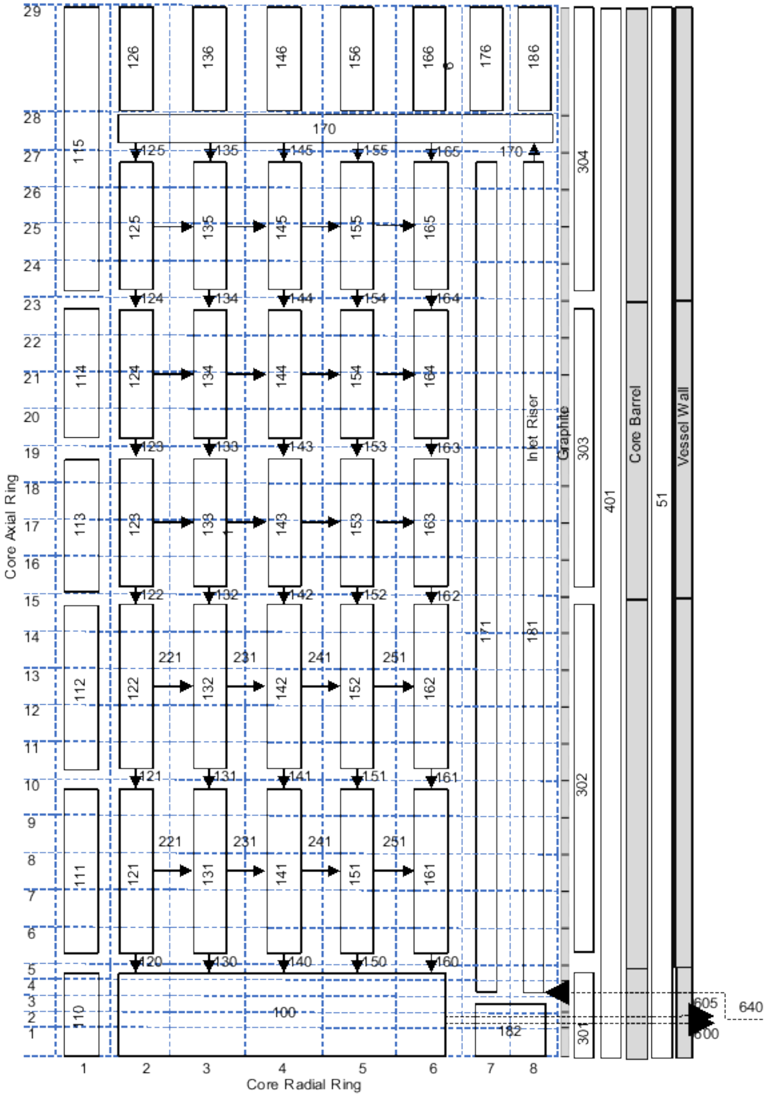

Vessel control volume, flow path, and heat structure nodalization with core package boundaries in blue

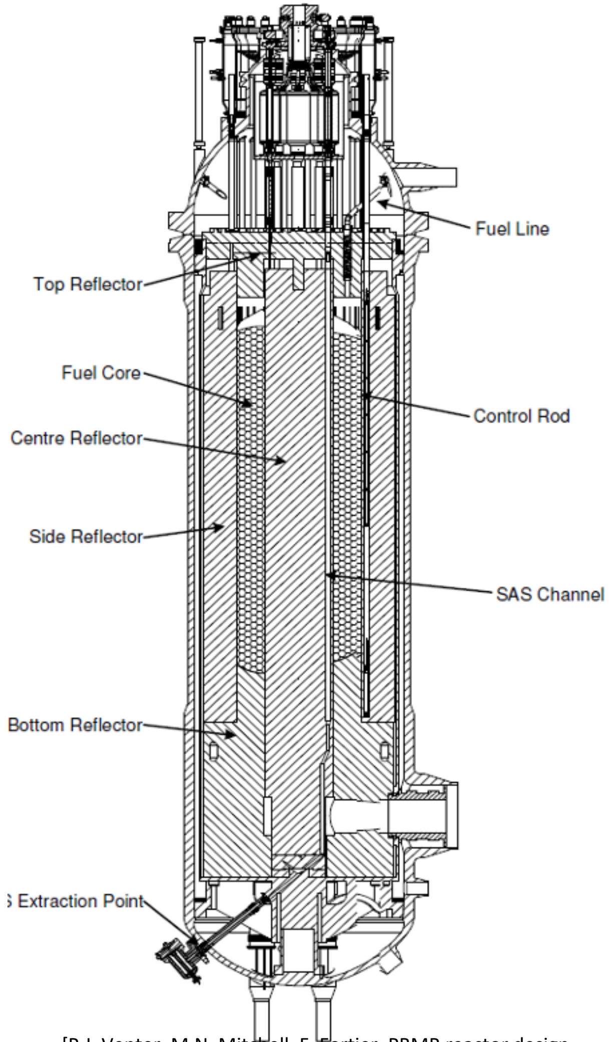

[P.J. Venter, M.N. Mitchell, F. Fortier, PBMR reactor design and development, in: Proceedings from the 18th International Conference on Structural Mechanics in Reactor Technology (SMiRT 18), Beijing, China, Aug. 2005]

Reactor building

- Nodalization guided by NGNP layout
  - Passive air-flow Reactor Cavity Cooling System (RCCS)
- Leakage assumed to be the same as BWR Mark I reactor building surrounding the containment
  - 100% vol/day at 0.25 psig

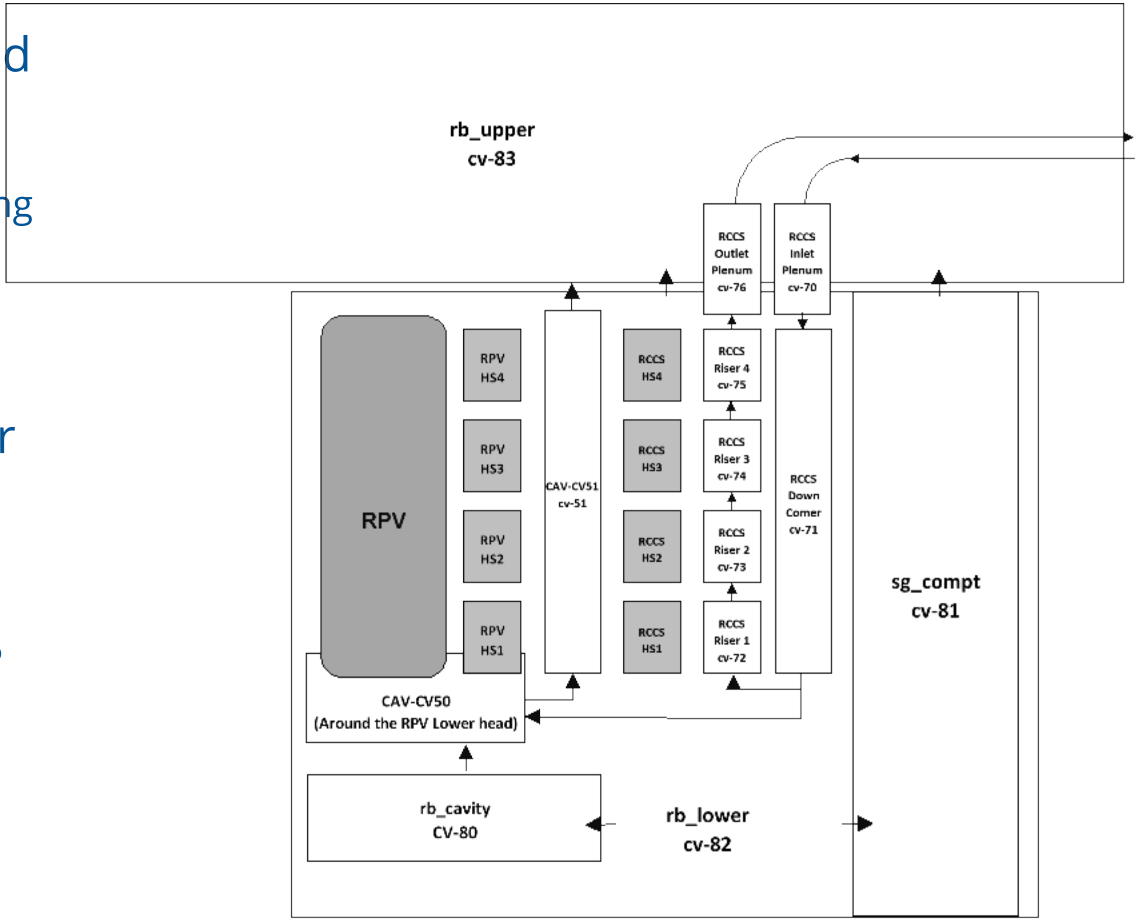

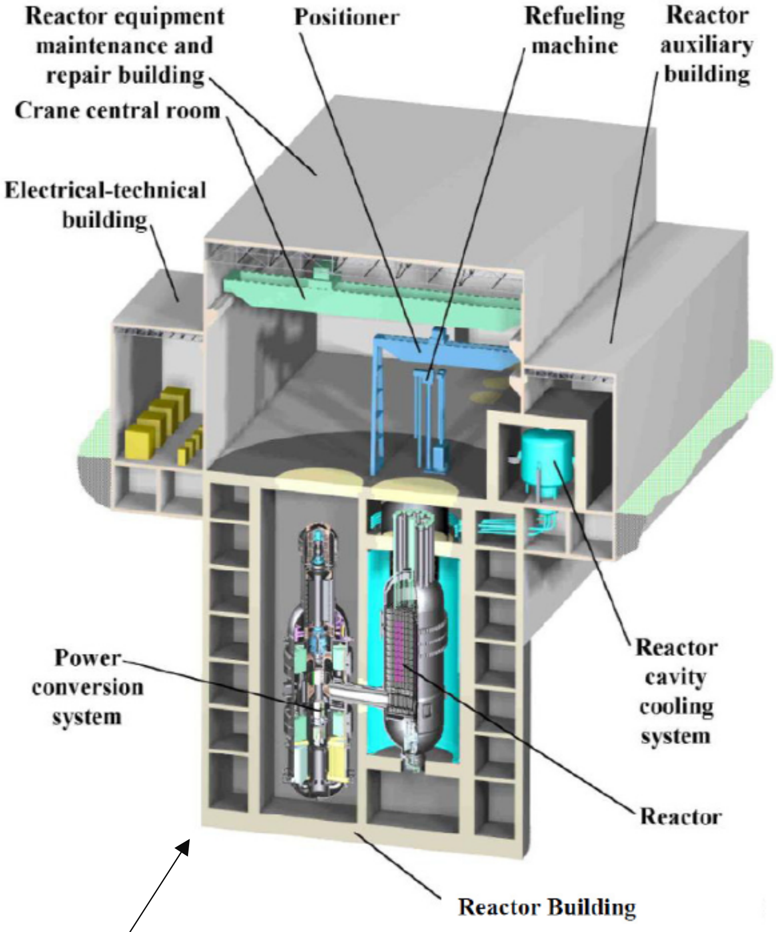

"HTGR Mechanistic Source Terms White Paper," July 2010, [INL-EXT-10-17999]

Picture above shows a water-cooled RCCS but demo model uses air-cooled RCCS.

Recirculation loop and secondary heat removal

MELCOR

Recirculation system and secondary heat removal

- Recirculation loop and secondary heat removal provide boundary conditions to the vessel
  - Flow rate
  - Heat removal & inlet temperature

Pipe break nodalization allows counter-current natural circulation flow

- MELCOR counter-current flow model used to represent adjacent stream drag forces
- Geometry similar to PWR hot leg natural circulation [NUREG-1922]
- Allows for air ingression

Scenario: depressurized loss of forced circulation (DLOFC)

- Assumes double-ended break of the hot leg

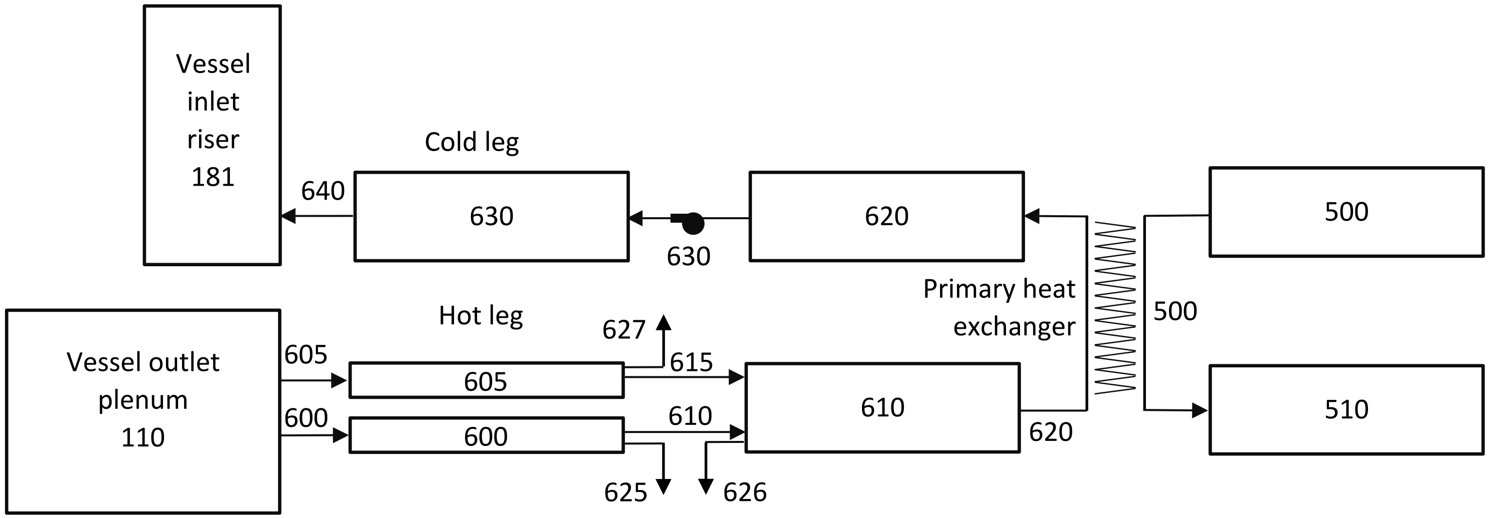

DLOFC scenario

DLOFC is initiated after 900 days of operation

- Long-term fission product concentrations developed in TRISO and pebble
- 24 kg/yr graphite dust generation based on German AVR experience
- TRISO initialized with 10^{-5} failure fraction during the steady state

Provisions for air ingression

Reactor cavity cooling system (RCCS) is operational

Individual sensitivity calculations to explore variations in the model response to uncertainty in input parameters

DLOFC reference case results (1/7)

Following pipe break

- Control rods insert to terminate fission
- The vessel depressurizes in seconds as the high-pressure helium escapes out both sides of the broken pipe
- Peak velocity in the pebble bed is 45 m/s (normal flow rate is 11-18 m/s)

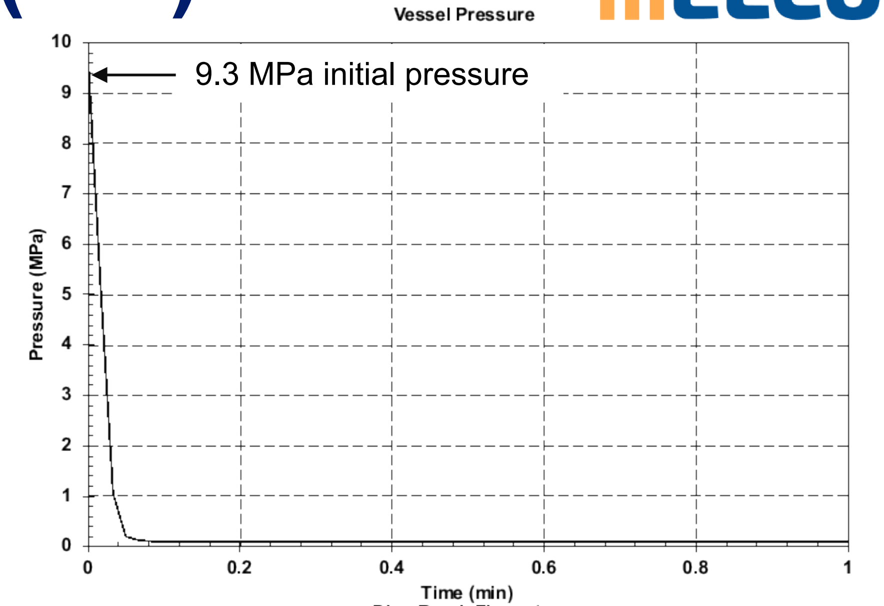

Counter-current flow established on the vessel side of the pipe break

- Hot gases from the exit plenum escape on the top side of the broken hot leg pipe and cooler gases enter along the bottom of the pipe

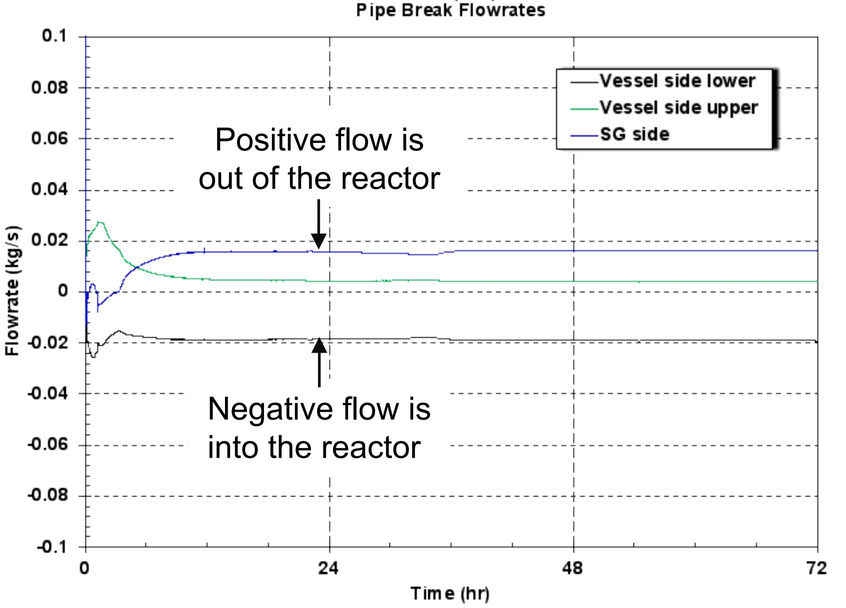

DLOFC reference case results (2/7)

In-vessel natural circulation flow after blowdown

- Upward flow in the inner region of the core where the fuel temperatures and decay power heating are higher
- Downward flow in the outer region of the core where the fuel temperatures and decay power heating are lower
- Flow increases when the fuel starts to cool

The fuel temperatures in the inner region of the pebble bed shift from cooler at inlet and hot at the outlet due to the flow reversal

- The axial fuel temperatures are affected by the local decay heat power (highest in the center) and the flow direction
  - During normal operation, the fuel at the exit (bottom) is the hottest
  - The exit becomes the coolest location (low power and cooler gases entering from the exit plenum)

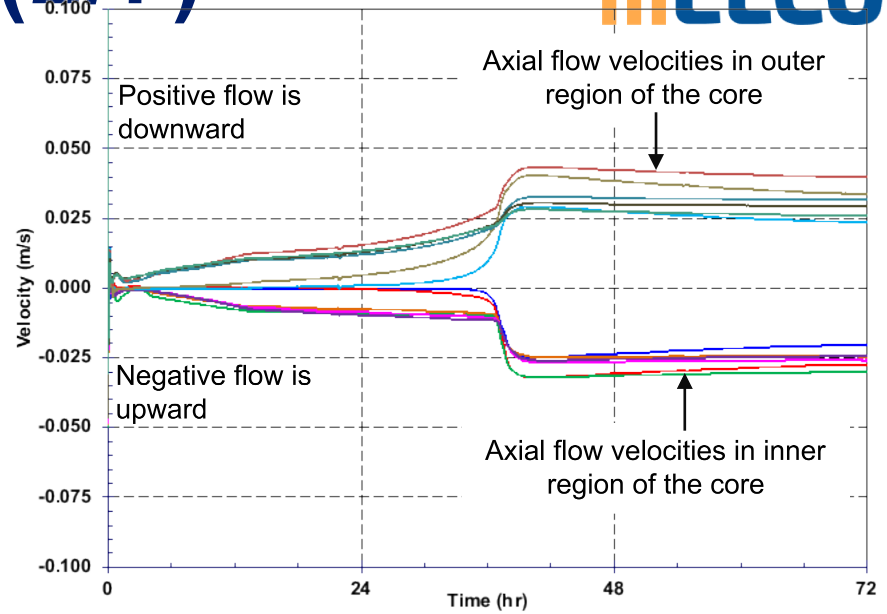

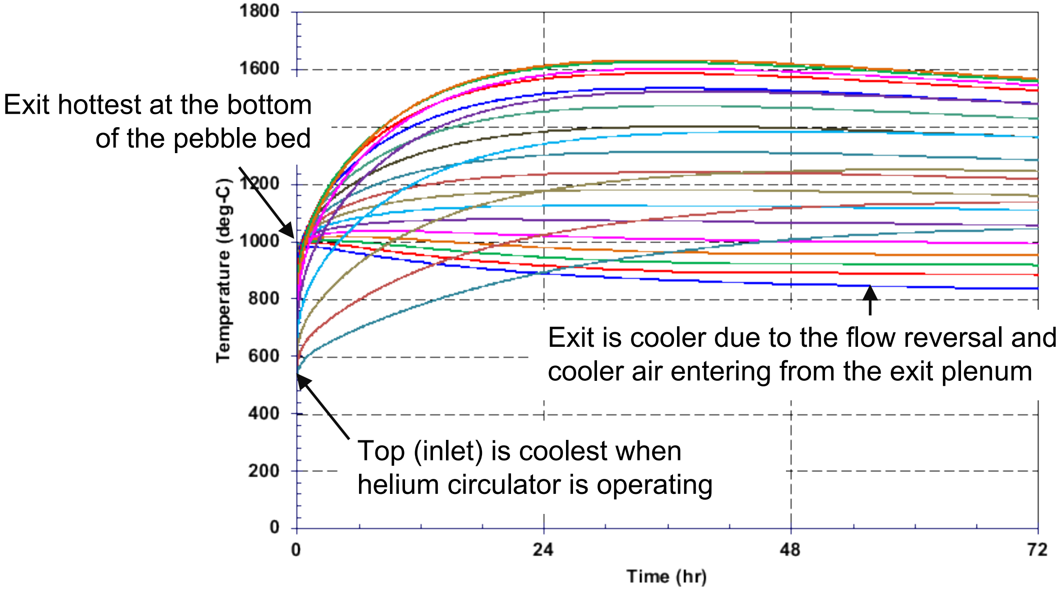

DLOFC reference case results (3/7)

The core heatup is dominated by the decay heat

- The air oxidation power is relatively small at <25 kW
- Although the vessel is thermally-stratified with a low exit path, a small natural circulation flow persists to bring air into the vessel
  - Pebble bed inlet and circulation velocities are <0.04 m/s

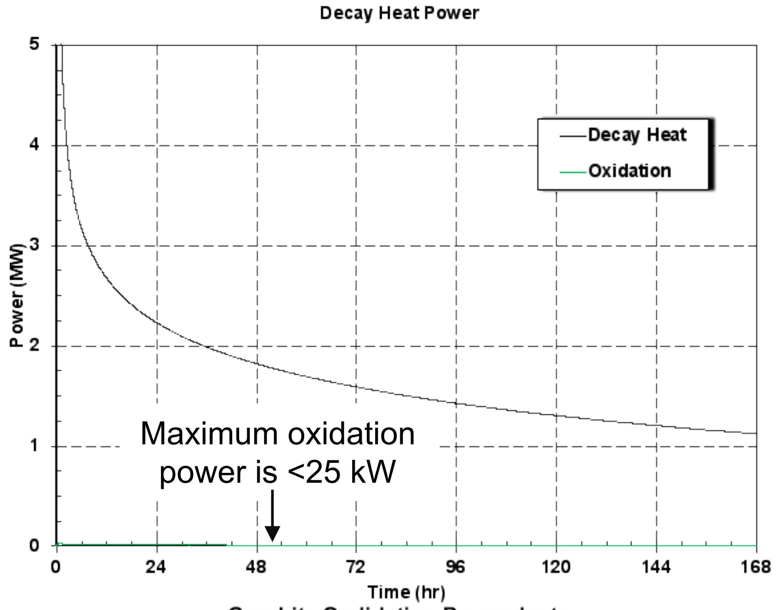

The graphite oxidation produces significant quantities of CO and CO_2

- Approximately 50% of the oxidation occurs in the graphite reflector structures around the inlet plenum and 50% in the lower portion of the pebble bed.
- ~1% of the pebble matrix oxidized after 168 hr
  - 17% peak pebble oxidation at the bottom center

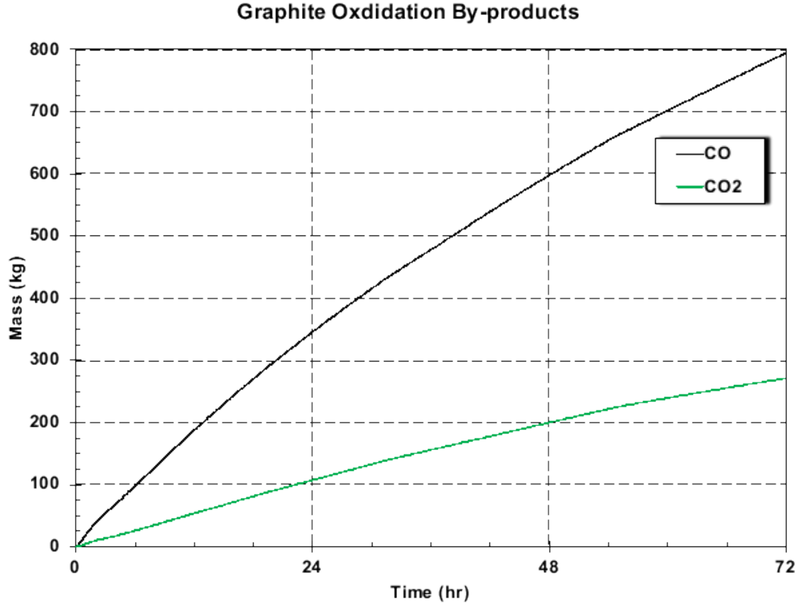

DLOFC reference case results (4/7)

MELCOR

Potential for combustion in the reactor building

- MELCOR lower limit for CO combustion with an ignition source is 12.9% (~2X higher than for hydrogen)
- Highly dependent on local concentrations and building design and interconnectivity
- Demo reactor building assumes high inter-connectivity
  - Allows air and CO circulation
- No carbon-dioxide burns were predicted through 168 hr

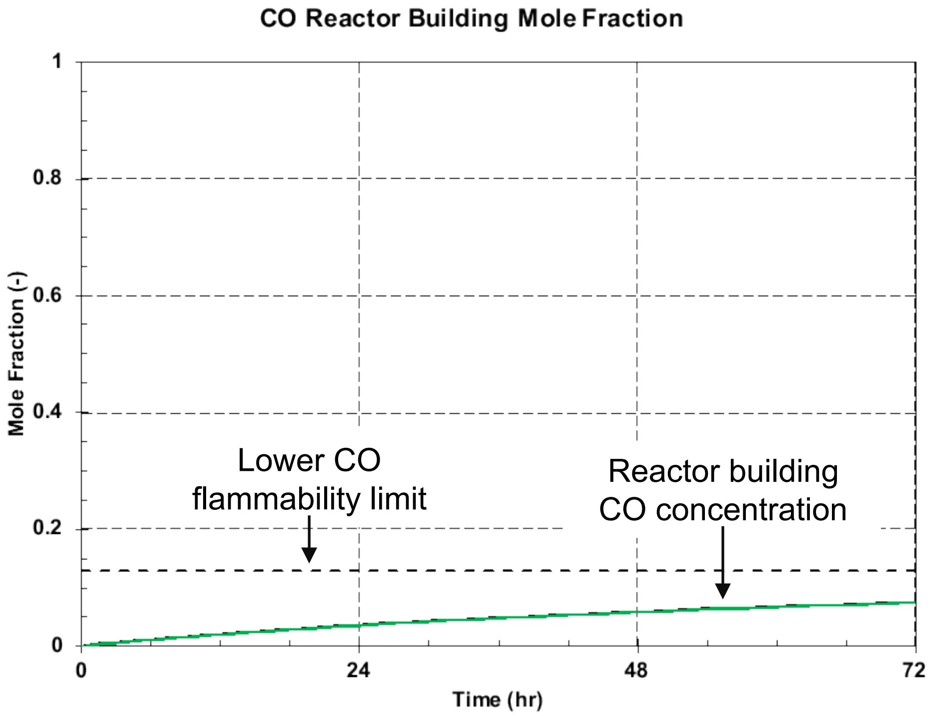

DLOFC reference case results (5/7)

MELCOR predicts release and transport from fuel to the environment

- Fuel heat-up
- TRISO layers – Initial failure fraction + failures during heat-up
- Pebble matrix and pebble outer shell – Higher diffusivity at elevated temperatures, recoil, and air oxidation
- Primary system – Failed with the initiating event
- Reactor building – Design leakage

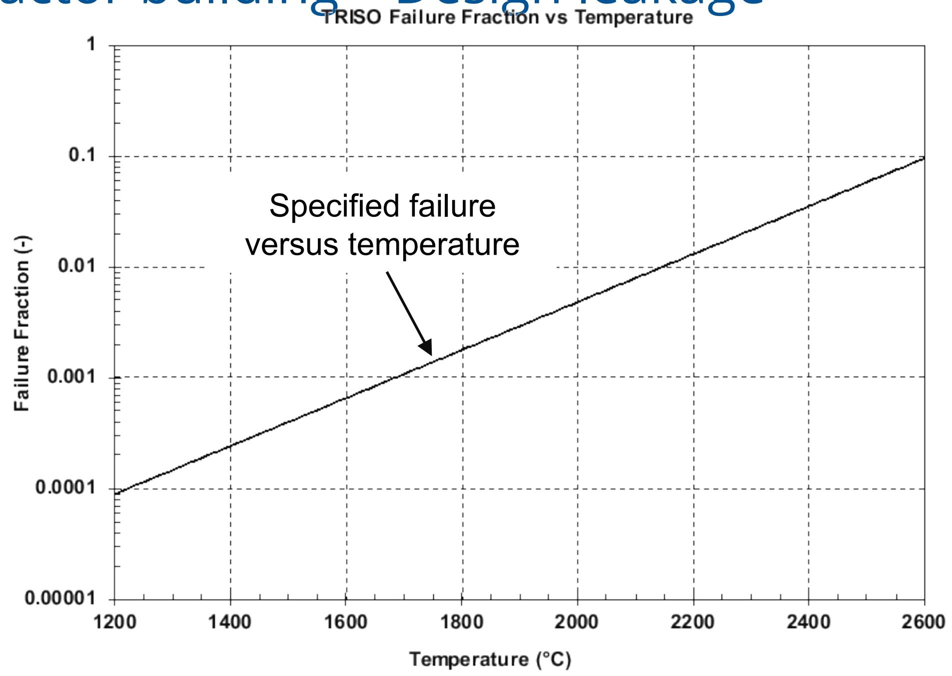

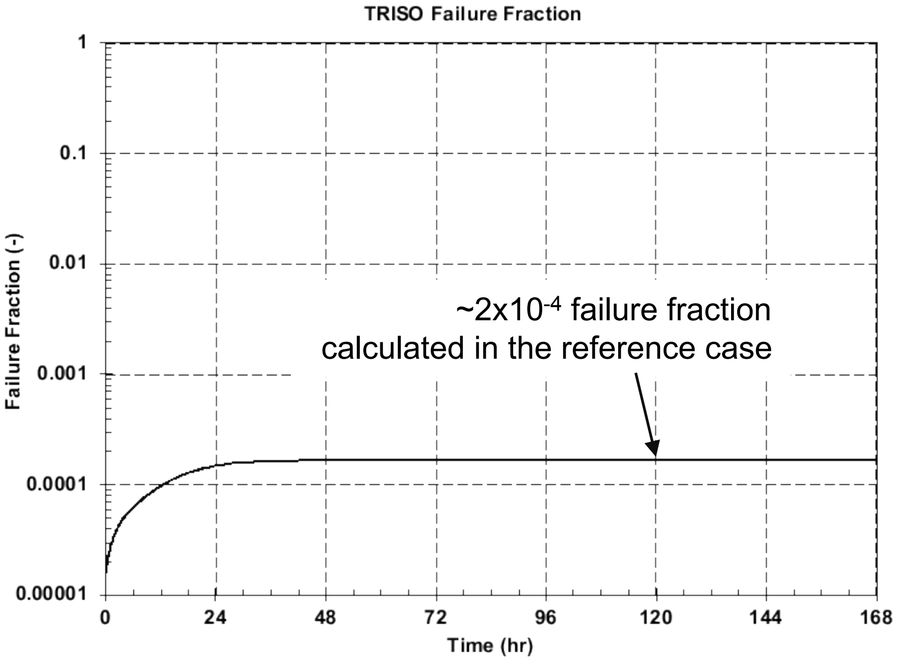

DLOFC reference case results (6/7)

The impact of the low TRISO failure fraction leads to small releases

- Iodine diffusivity assumed to be same as krypton
- Assumes most iodine reacts with cesium
- Larger cesium release due its the higher diffusivity
- Ag release to the environment is 1.2×10^{-3} (highest diffusivity)

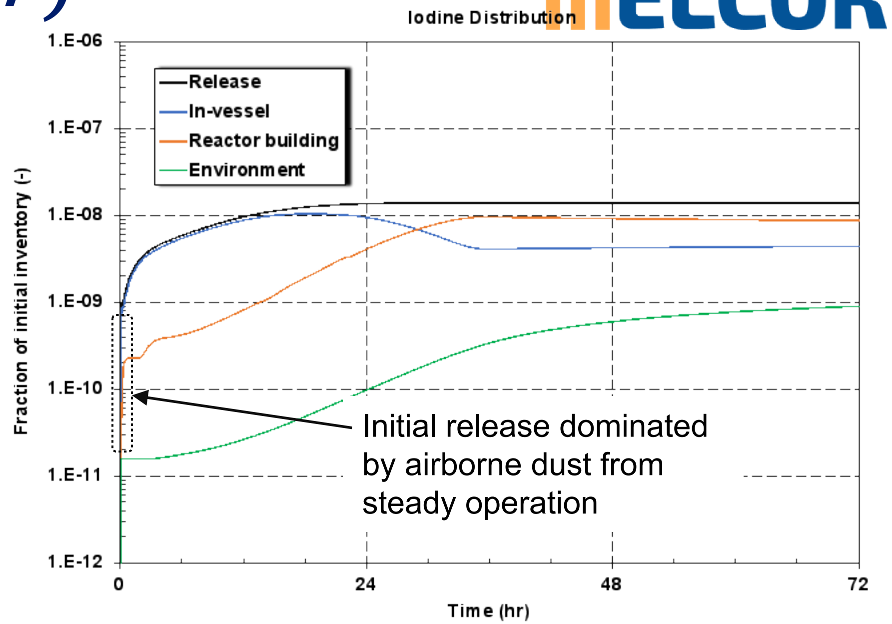

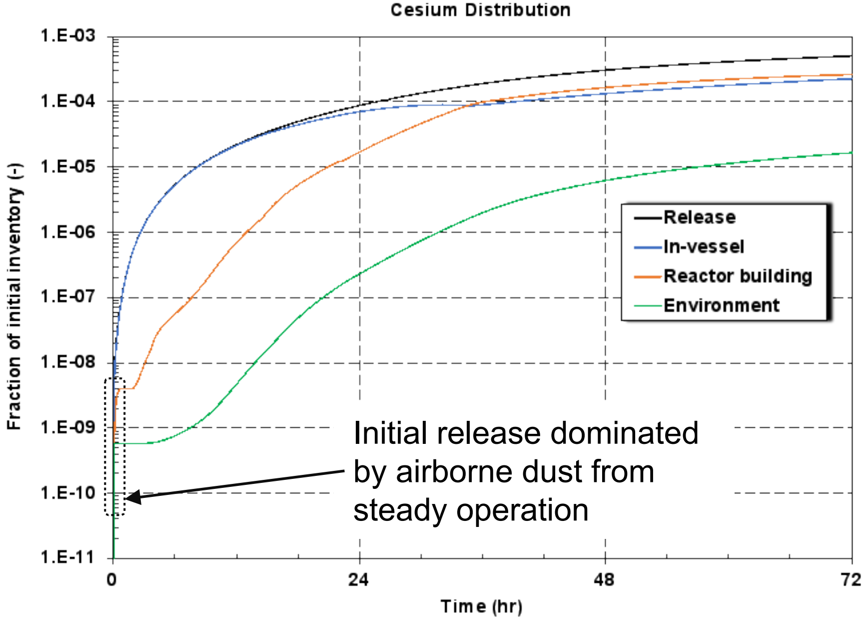

DLOFC reference case results (7/7)

Of the small release from the fuel…

34% and 62% of iodine and cesium, respectively, retained in the vessel

- Thermally-stratified orientation limits vessel releases
- Low flowrate combined with aerosol deposition
- Inclusion of graphite oxidation reaction products (CO and CO_2) promotes more flow and therefore more releases from the vessel

58% and 34% of iodine and cesium, respectively, retained in the reactor building

- No strong driving force for reactor building leakage
  - Reference model uses a hole size equivalent to 100% leakage per day at a design pressure of 0.25 psig (3.2 in^2)

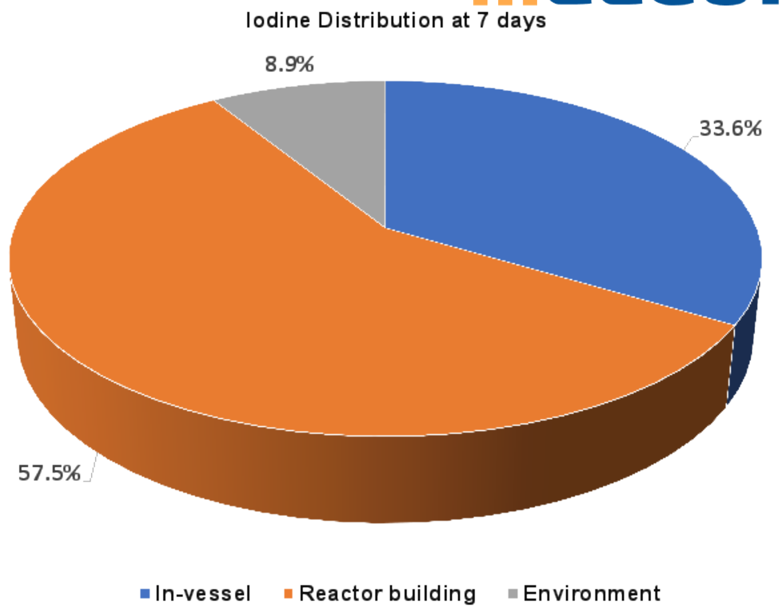

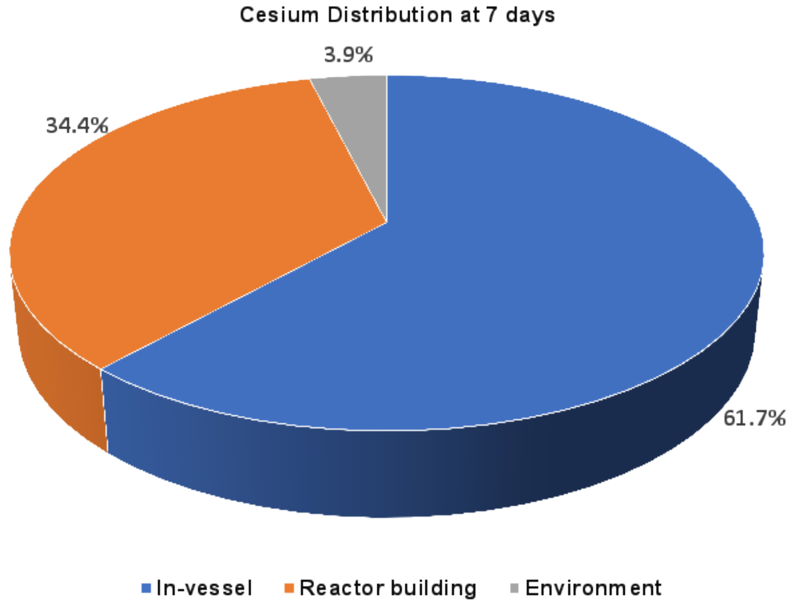

MELCOR can be used to explore the variability of the results to uncertainties

Model	Parameter	Distribution	Range
TRISO Model Parameters	Initial TRISO Failure Fraction (fraction of inventory)	Log uniform	$10^{-5} – 10^{-3}$
	TRISO Failure Rate Multiplier (-)	Log uniform	0.1 – 10.0
	Intact TRISO Diffusivity Multiplier (-)	Log uniform	0.001 – 1000.0
	Failed TRISO Diffusivity Multiplier (-)	Log uniform	0.001 – 1000.0
	Matrix Diffusivity Multiplier (-)	Log uniform	0.001 – 1000.0
	TRISO Pebble Emissivity (-)	Uniform	0.5 – 0.999
	TRISO Pebble Bed Porosity (-)	Uniform	0.3 – 0.5
	TRISO recoil fraction (-)	Uniform	0 – 0.03
Radionuclide Model Parameters	Shape Factor (-)	Uniform	1.0 – 5.0
	Gaseous Iodine Multiplier (Base = 5% I_2)	Uniform	0.02 – 1.0
Design Parameters	Graphite Conductivity Multiplier (-)	Uniform	0.5 – 1.5
	Decay Heat Multiplier (-)	Uniform	0.9 – 1.1
	RCCS Blockage Multiplier (-)	Log uniform	0.001 – 1.0
	RCCS Emissivity (-)	Uniform	0.1 – 1.0
	Reactor Building Leakage Multiplier (-)	Log uniform	0.1 – 100.0
	Wind speed (m/s)	Uniform	0 - 10

Single parameter sensitivity results (1/4)

ELCOR

The sensitivity parameters were sampled at the minimum and maximum values to illustrate their impacts

- A low graphite conductivity has the largest impact on the peak fuel temperature
  - Graphite conductivity varies considerably with irradiation (>10X) and also varies with temperature
- ±10% decay heat has next largest impact on the peak fuel temperature
- High/low emissivity, the next most important single factor, is used as a surrogate for the relative importance of radiative exchange in the pebble bed
- Debris bed porosity had a small effect on the peak fuel temperature
- Heat dissipation limits the magnitude of the initial peak for a blocked RCCS
  - Slow heat-up to 1800°C by 7 days

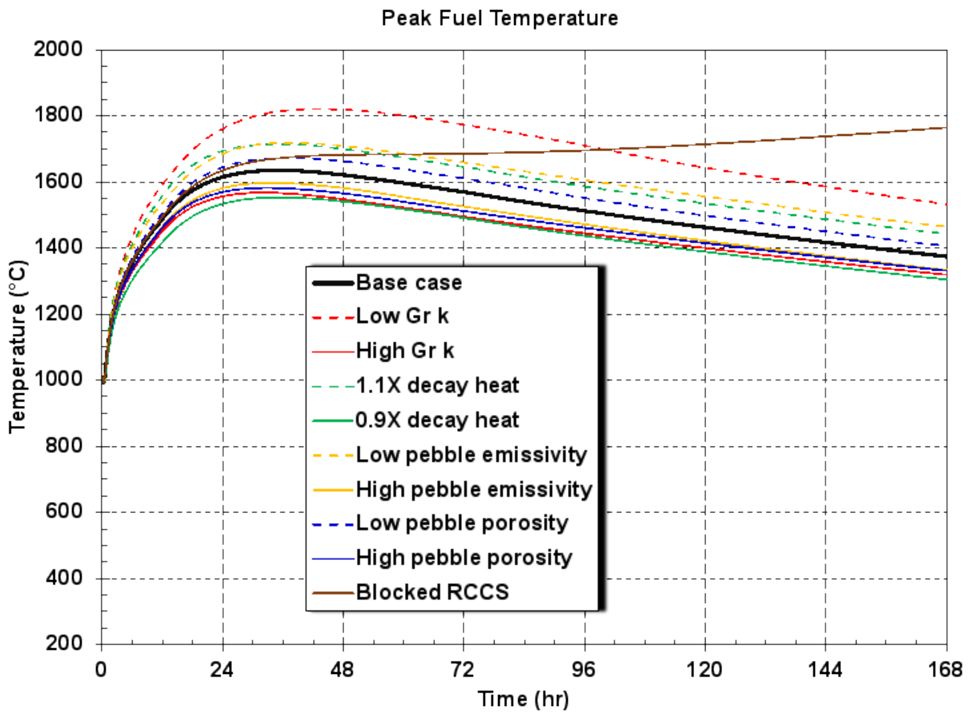

Examples of single parameter sensitivity results (2/4)

As the peak fuel temperature rises, the TRISO failure fraction increases

- Blocked RCCS does not have impact for several days

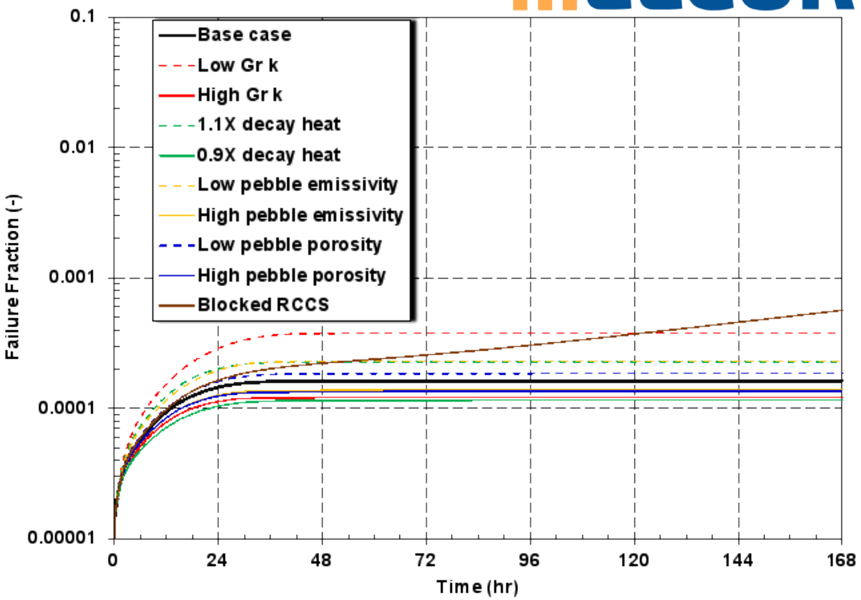

The cesium environmental release shows an order of magnitude variation

- Reflects variations in release from the pebbles
- Graphite conductivity had the largest impact
- Variations in emissivity = uncertainty in radiative heat transport (similar to ±10% in decay heat power)
- Pebble porosity had a small impact

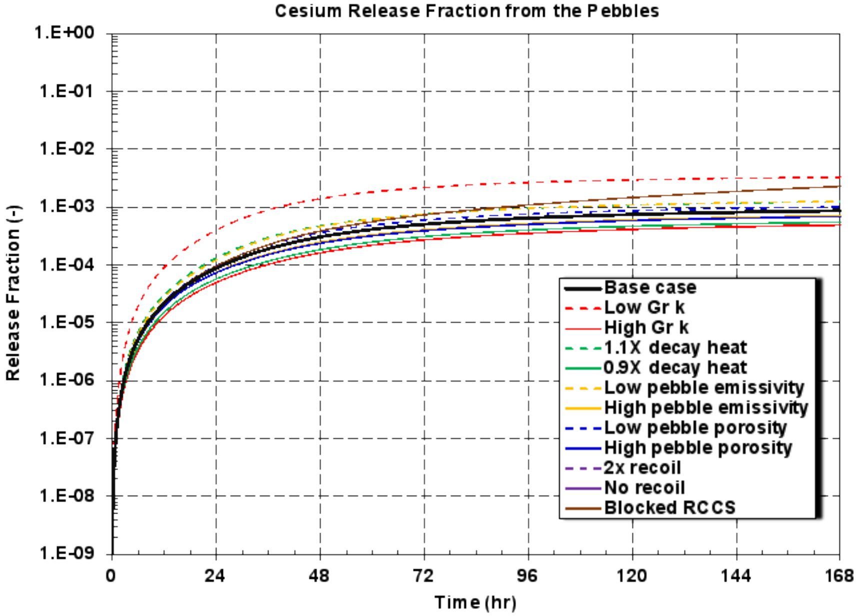

Examples of single parameter sensitivity results (3/4)

Larger hole size in the building and higher wind speed causes higher releases to environment

- 100X building leakage has less than a 10X impact
- External wind has small effect

Graphite oxidation and the associated CO/CO_2 production did not increase the source term

- CO/CO_2 gas production did not increase environment release

Early impacts of the recoil and initial TRISO failure fraction did not impact long-term environmental release

- Magnitude of the release dominated by the fuel temperature response and the TRISO failure model

Late step change in the blocked RCCS release is due to a carbon monoxide burn

- Building pressurization forces out airborne radionuclides

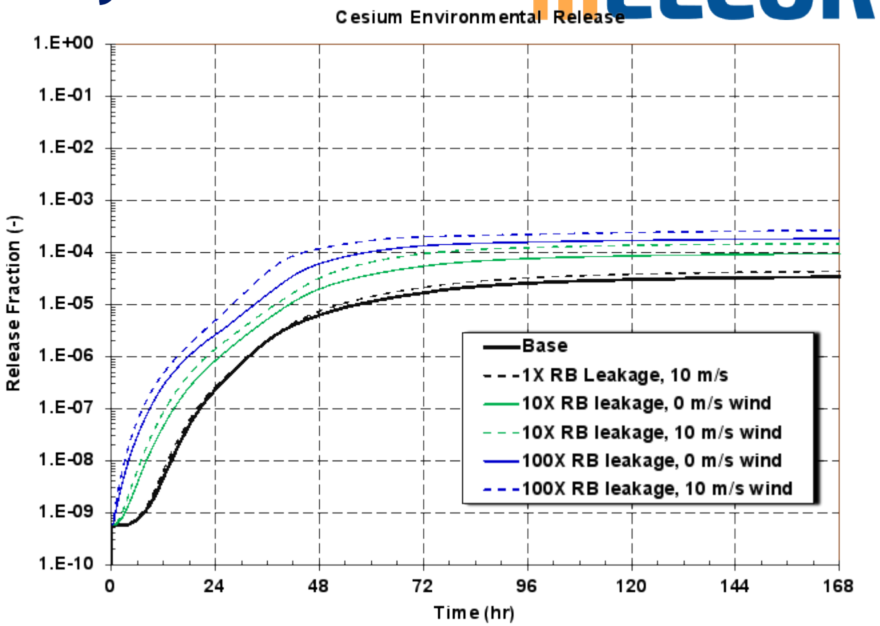

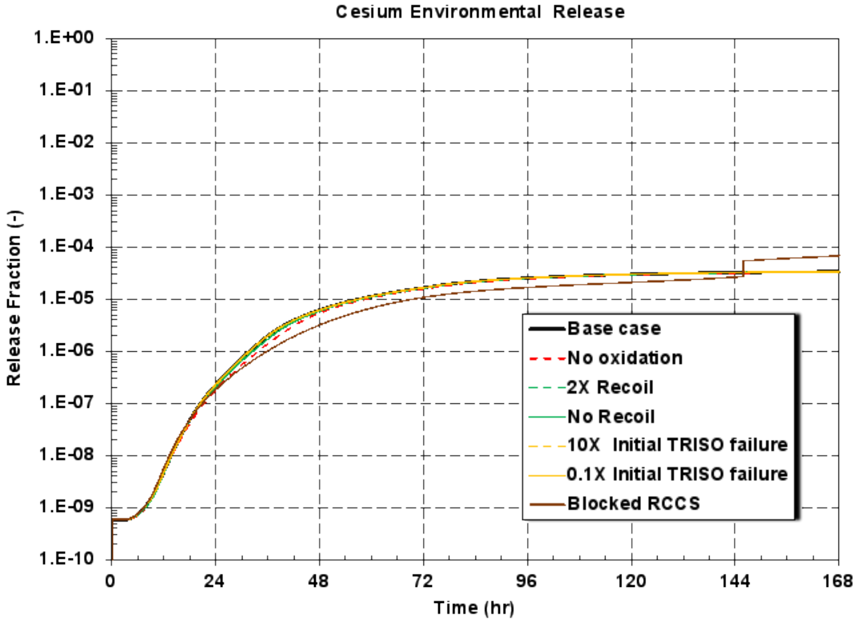

Examples of single parameter sensitivity results (4/4)

Blocked RCCS leads to higher CO generation

- Ratio of reaction products is dependent on the temperature of the graphite
- Blocked RCCS generates ~9% more moles of CO and CO_2

Higher CO generation led to a burn in the steam generator compartment (pipe break location)

- Incomplete burn with slow flame speed
  - Low oxygen concentration (6.8%)
- 0.25 bar (3.5 psi) pressure rise
- Burn creates non-condensable CO_2
  - No subsequent condensation

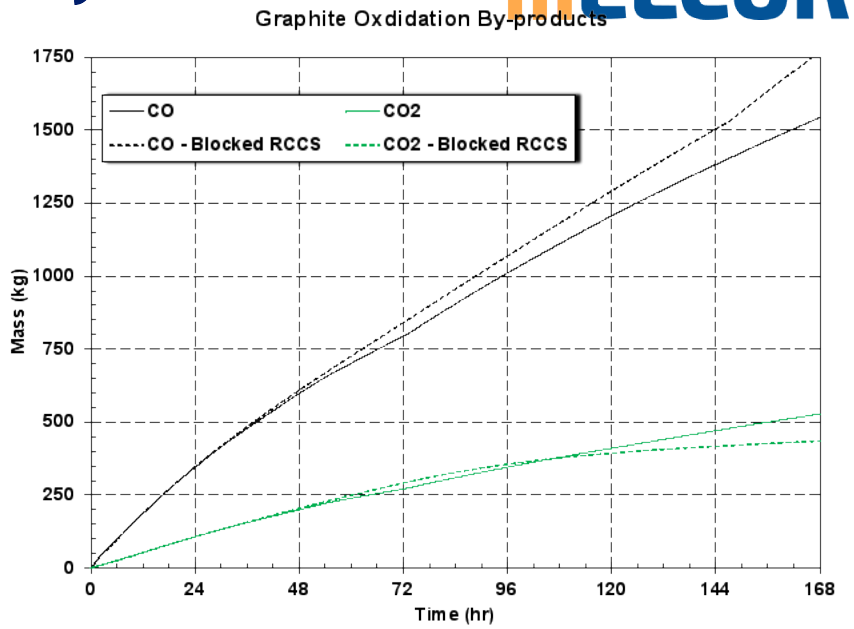

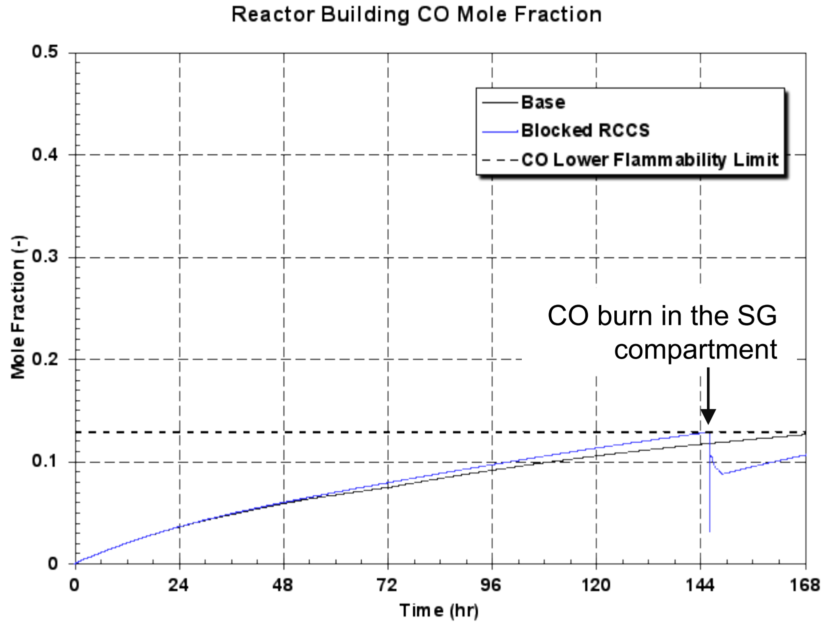

UO_2 Thermal Response

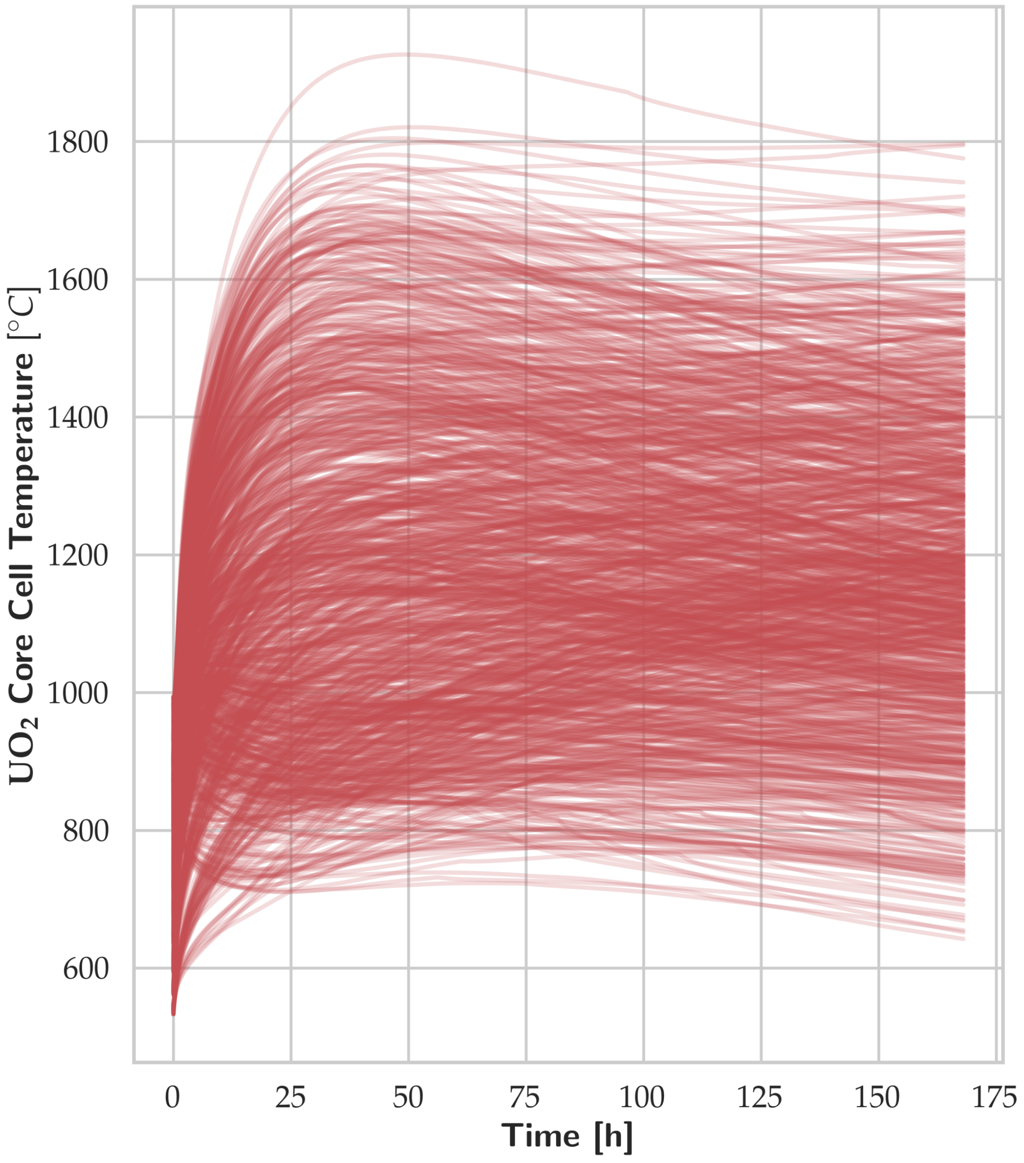

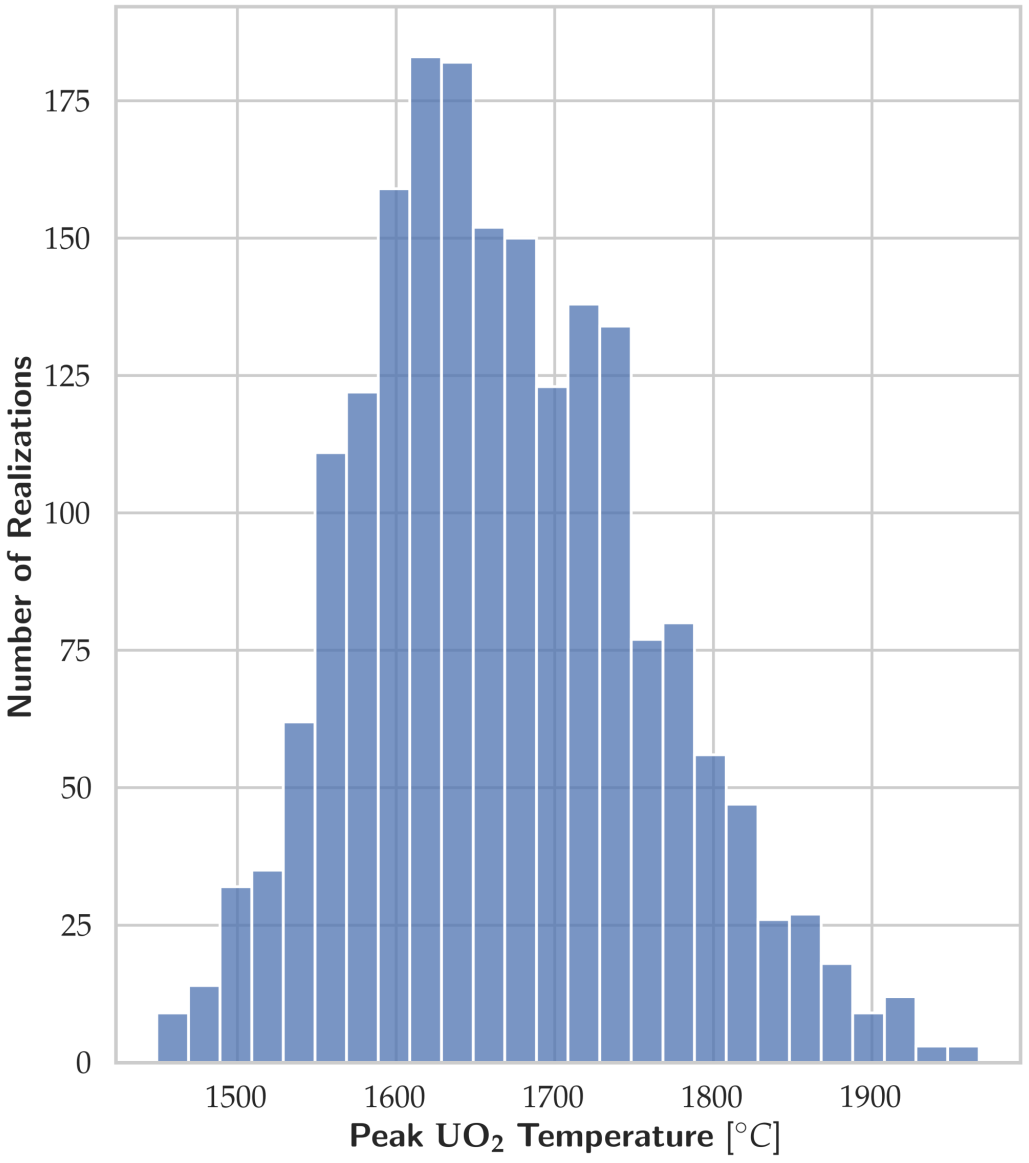

UO_2 Thermal Transient Evolution

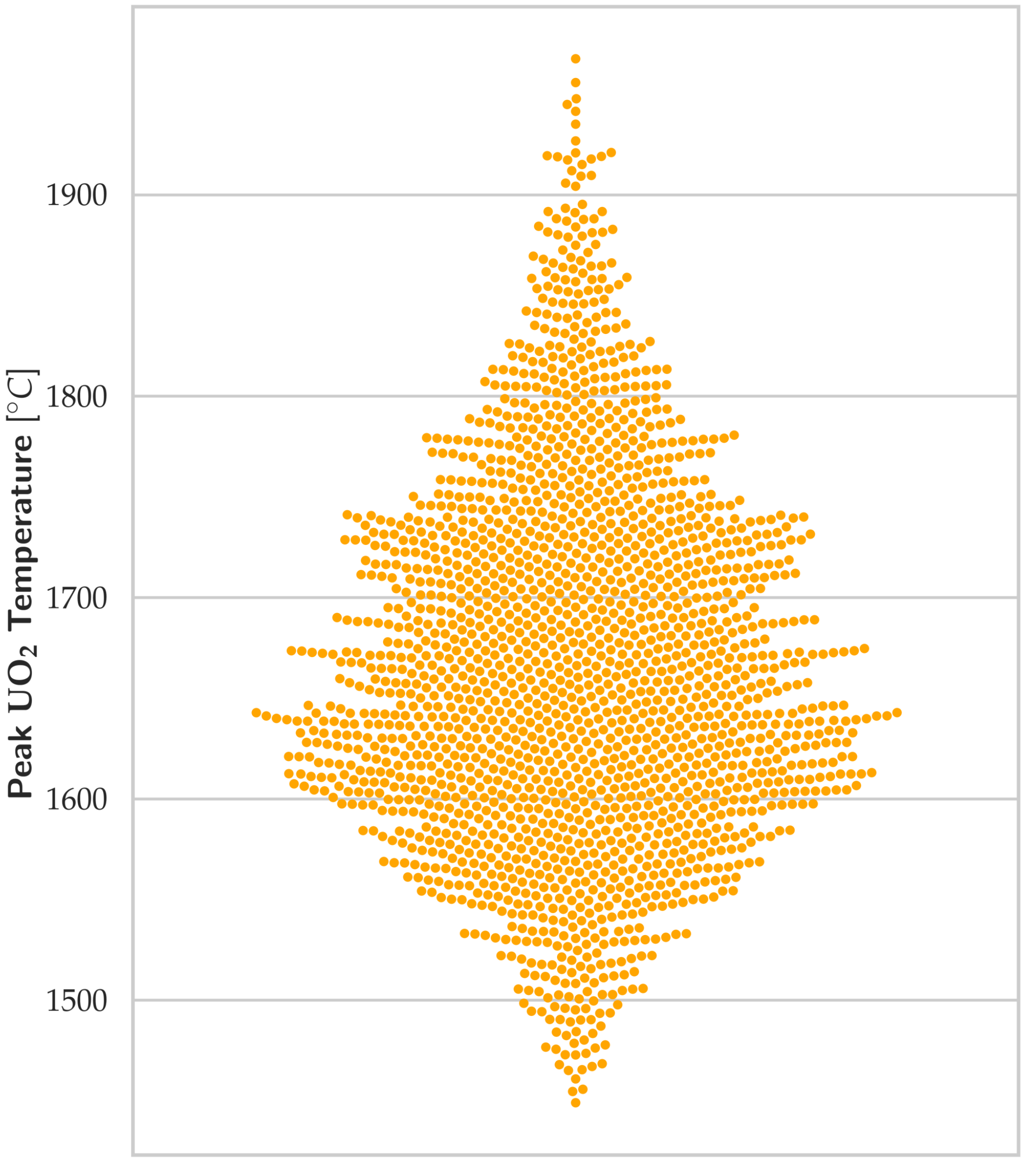

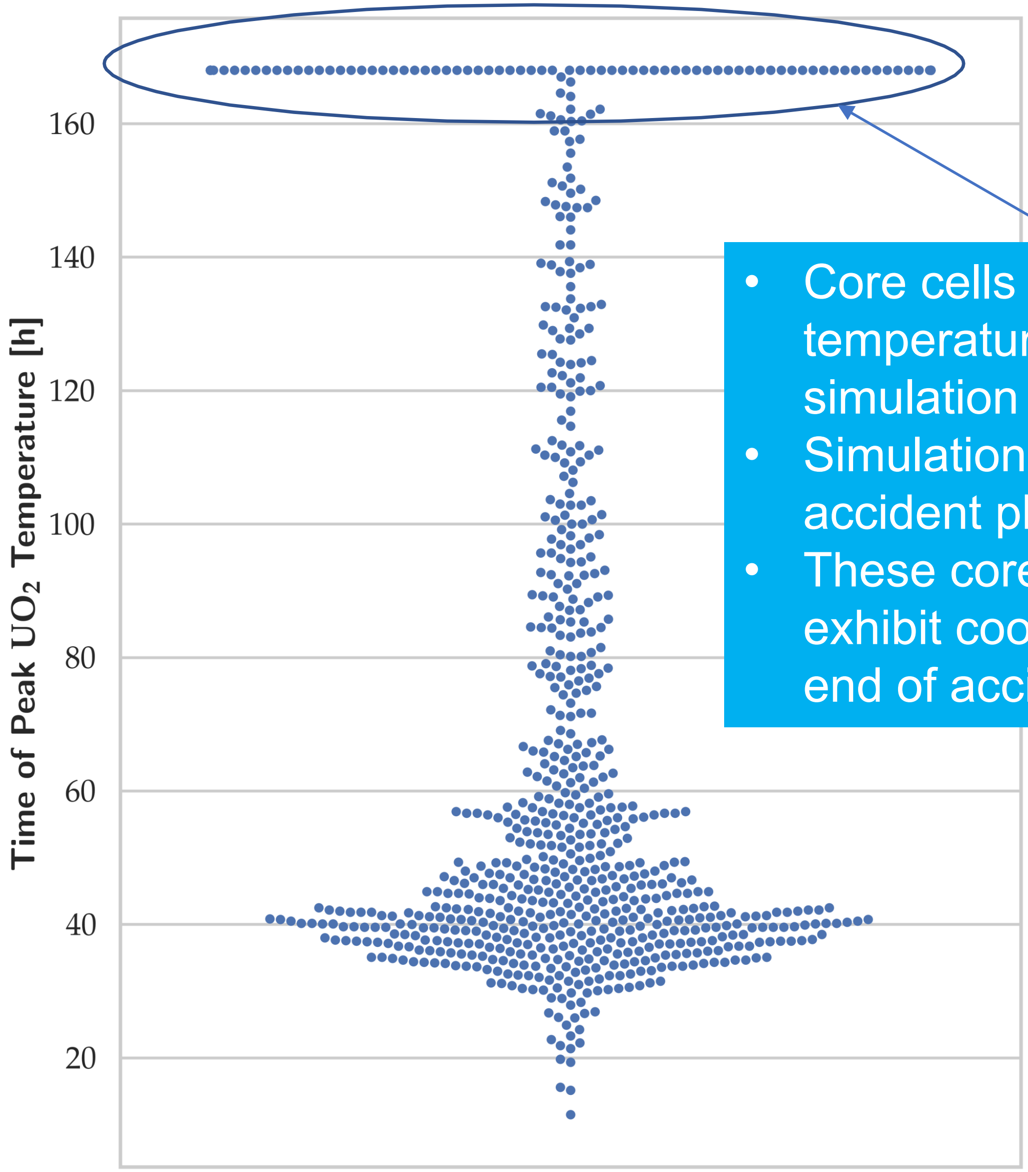

- Core cells with peak fuel temperatures at end of simulation
- Simulation time denoted as accident phase
- These core cells do not exhibit cooldown prior to end of accident phase

TRISO Particle Failure

Long-term TRISO particle failure possible for core cells exhibiting prolonged over-temperatures

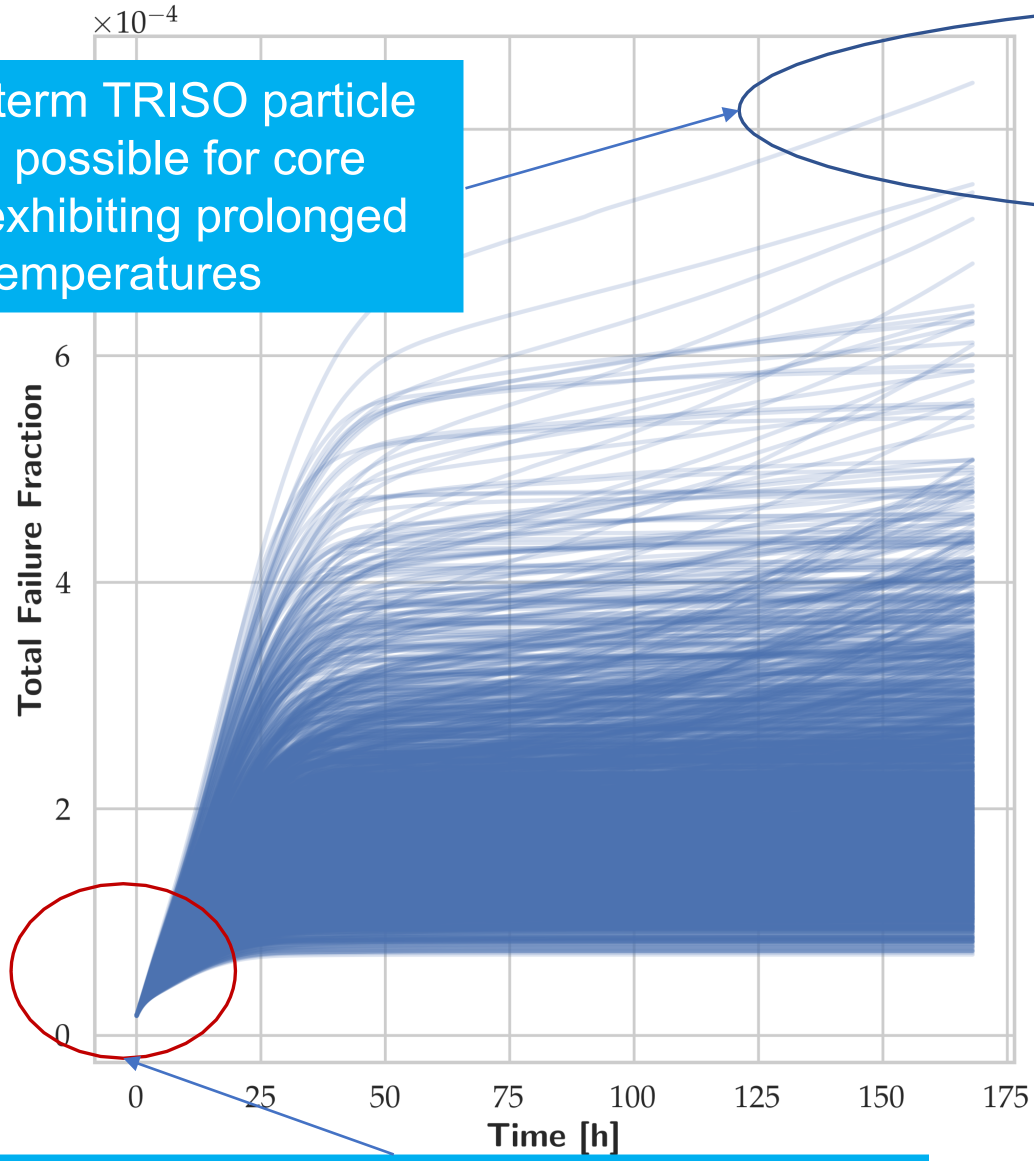

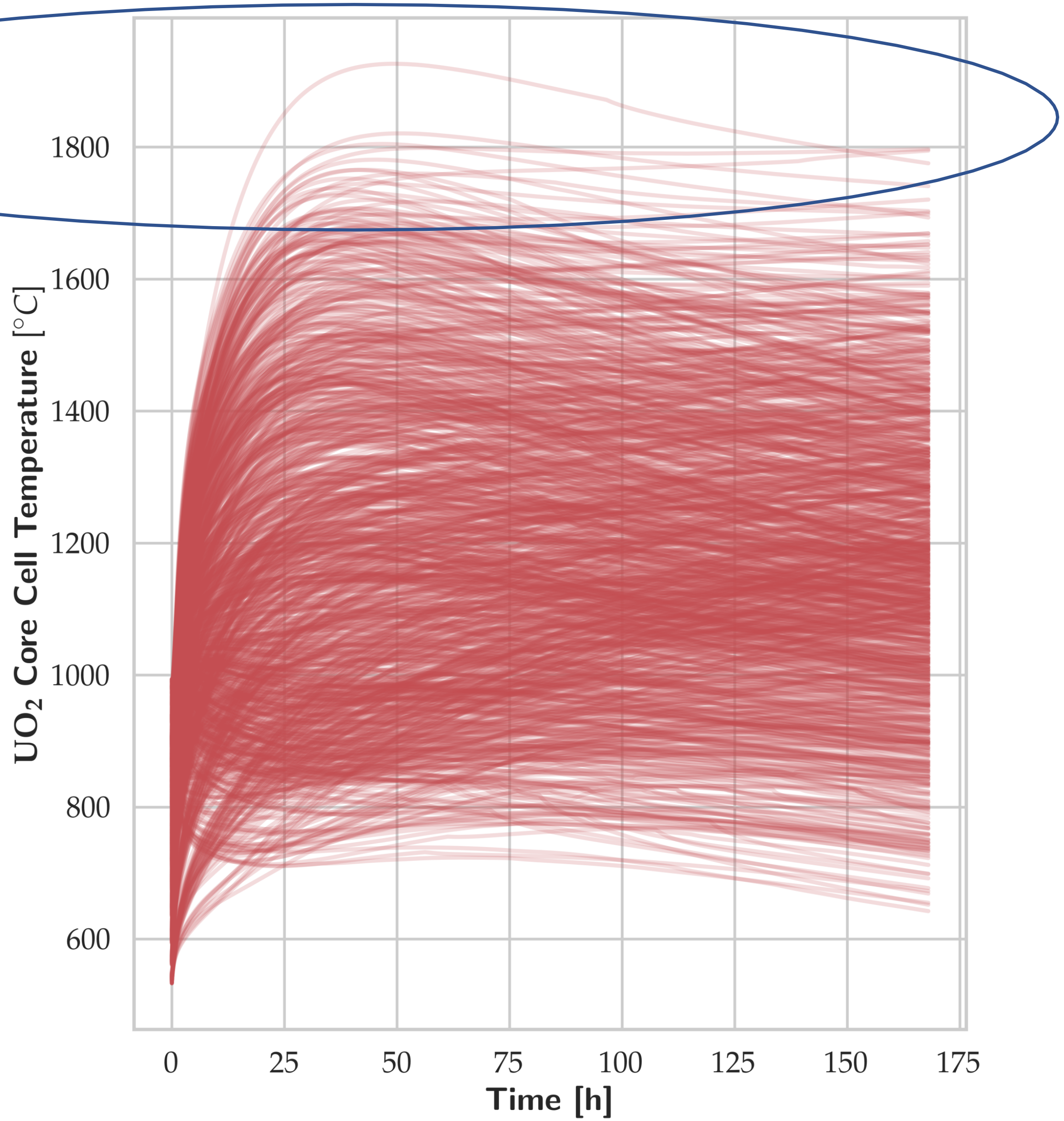

Initial distribution of failed TRISO particles

Evolution of TRISO Particle Failures

ELCOR

Long-term failures of TRISO particles at lower rate but driven by prolonged period of elevated fuel temperature

Rapid growth in failure fraction driven by the early temperature excursion

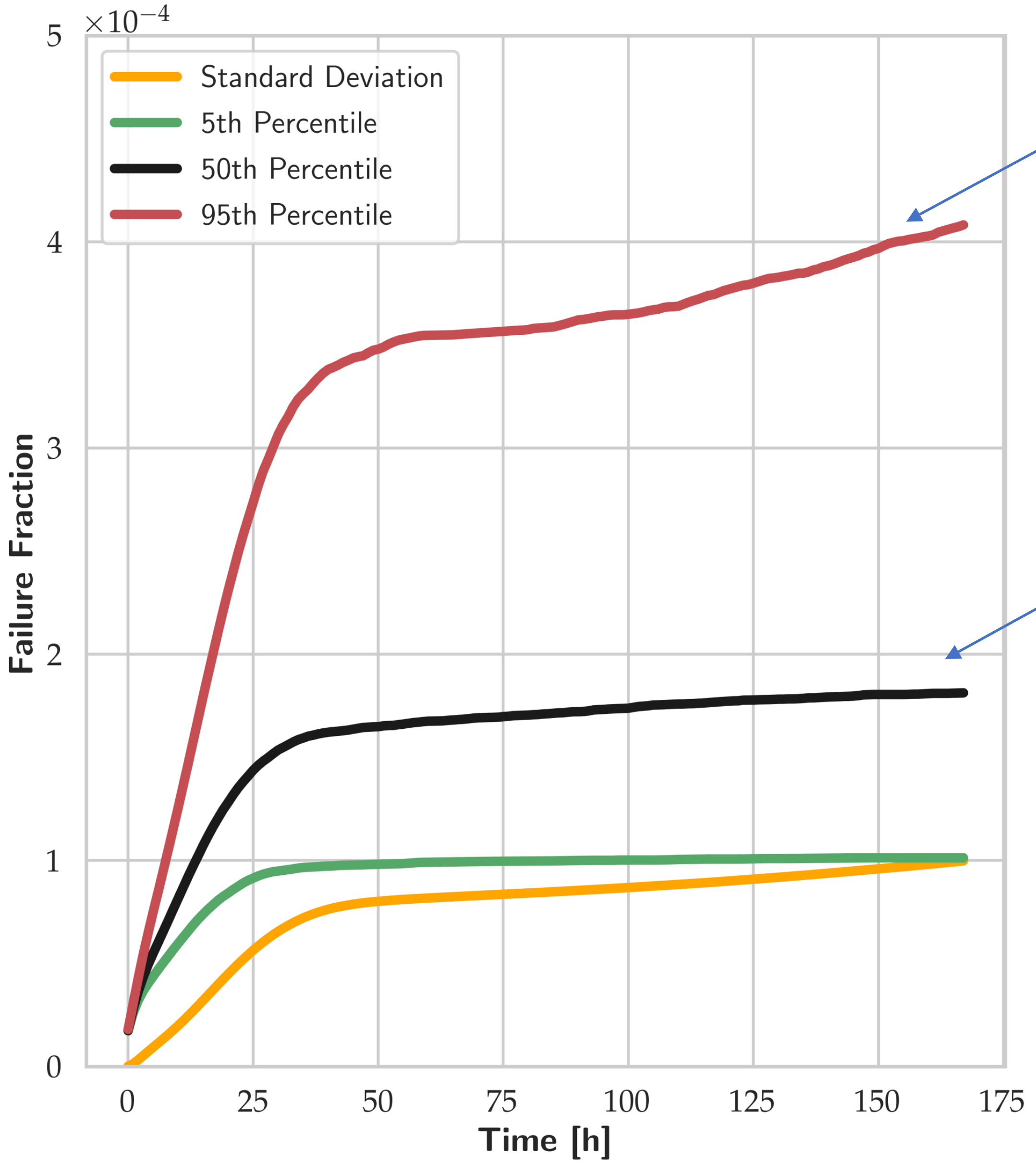

Tails of realizations contributing to longer term growth of TRISO particle failures

50th percentile reasonably stable in the long-term

Lower rates of failure entirely driven by early temperature excursion

Variability in peak fuel temperature and cooldown transient dominates higher failure rate realizations

Role of Decay Heat Rejection – Latest Time to Peak Fuel Temperature

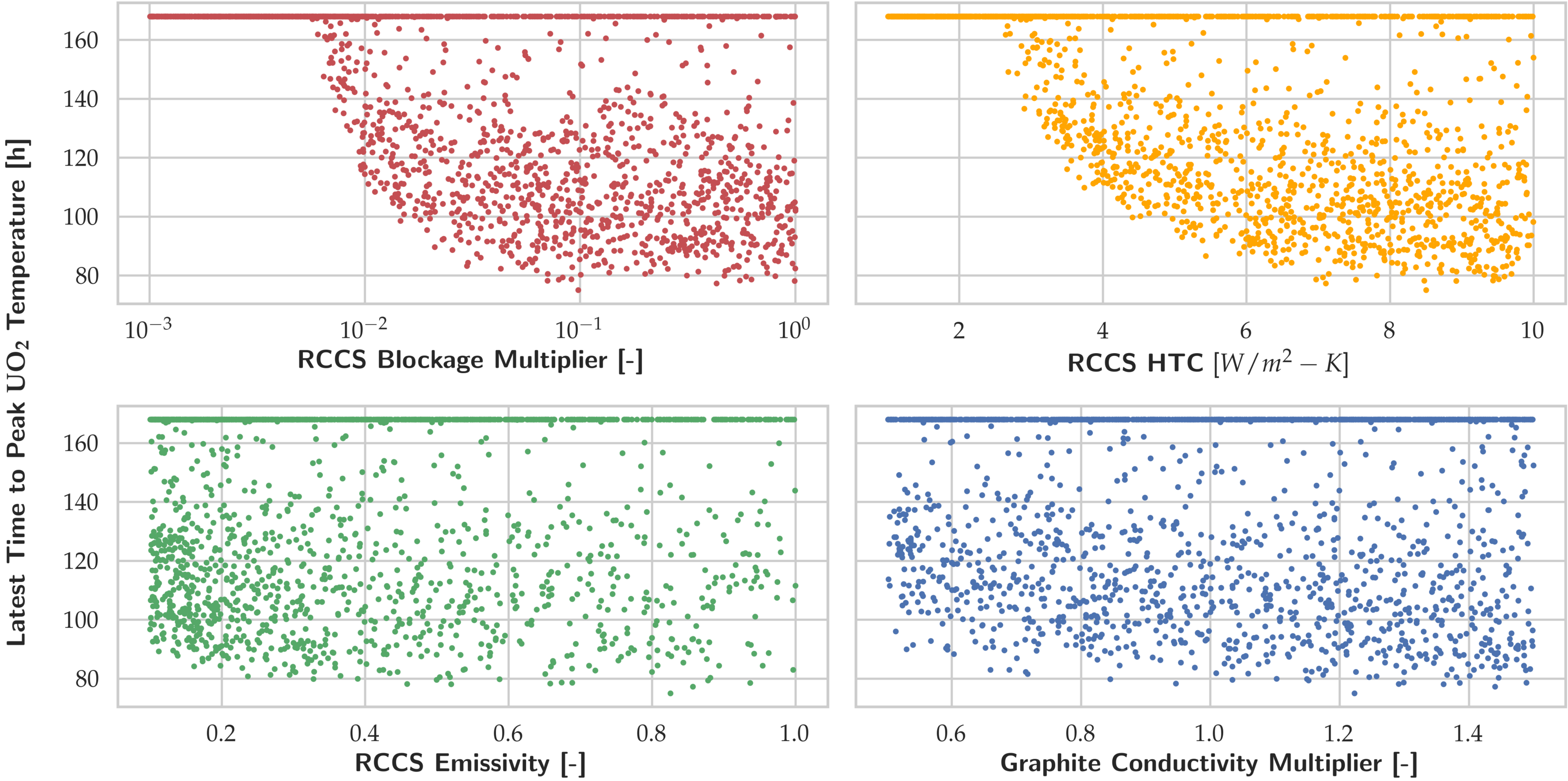

Role of Decay Heat Rejection – Peak Fuel Temperature